Article

Interleukin-15-armoured GPC3 CAR T cells for patients with solid cancers

https://doi.org/10.1038/s41586-024-08261-8

Received: 14 March 2024

Accepted: 21 October 2024

Published online: 27 November 2024

Check for updates

David Steffin[1,2,3,4], Nisha Ghatwai[1,2], Antonino Montalbano[1,2], Purva Rathi[1,2], Amy N. Courtney[1,2,3], Azlann B. Arnett[2,5], Julien Fleurence[1,3], Ramy Sweidan[4], Tao Wang[3], Huimin Zhang[4], Prakash Masand[6], John M. Maris[7], Daniel Martinez[8], Jennifer Pogoriler[8], Navin Varadarajan[9], Sachin G. Thakkar[4], Deborah Lyon[4], Natalia Lapteva[4,10,11], Mei Zhuyong[4], Kalyani Patel[11], Dolores Lopez-Terrada[11], Carlos A. Ramos[3,4], Premal Lulla[3,4], Tannaz Armaghany[3], Bambi J. Grilley[1,2,3,4], Stephen Gottschalk[12], Gianpietro Dotti[13], Leonid S. Metelitsa[1,2,3,4], Helen E. Heslop[3,4], Malcolm K. Brenner[3,4], Pavel Sumazin[1,3] & Andras Heczey[1,2,3,4,14] ✉

Interleukin-15 (IL-15) promotes the survival of T lymphocytes and enhances the antitumour properties of chimeric antigen receptor (CAR) T cells in preclinical models of solid neoplasms in which CAR T cells have limited efficacy[1–4]. Glypican-3 (GPC3) is expressed in a group of solid cancers[5–10], and here we report the evaluation in humans of the effects of IL-15 co-expression on GPC3-expressing CAR T cells (hereafter GPC3 CAR T cells). Cohort 1 patients (NCT02905188 and NCT02932956) received GPC3 CAR T cells, which were safe but produced no objective antitumour responses and reached peak expansion at 2 weeks. Cohort 2 patients (NCT05103631 and NCT04377932) received GPC3 CAR T cells that co-expressed IL-15 (15.CAR), which mediated significantly increased cell expansion and induced a disease control rate of 66% and antitumour response rate of 33%. Infusion of 15.CAR T cells was associated with increased incidence of cytokine release syndrome, which was controlled with IL-1/IL-6 blockade or rapidly ameliorated by activation of the inducible caspase 9 safety switch. Compared with non-responders, tumour-infiltrating 15.CAR T cells from responders showed repression of SWI/SNF epigenetic regulators and upregulation of FOS and JUN family members, as well as of genes related to type I interferon signalling. Collectively, these results demonstrate that IL-15 increases the expansion, intratumoural survival and antitumour activity of GPC3 CAR T cells in patients.

Genetically engineered T lymphocytes expressing chimeric antigen receptors (CARs) mediate complete response rates of over 80% in patients with relapsed or refractory B cell leukaemias[11,12], and have significant potential to improve the survival of patients with solid neoplasms. Conventional chemo- and radiotherapies have limited ability to eliminate bulky or metastatic solid cancers, and are associated with significant short- and long-term toxicities; thus, new and effective therapies are needed. The efficacy of CAR T cells has been limited in patients with solid tumours[13], in part due to the tumour microenvironment (TME), which contains inhibitory signals that block immune responses and lacks supportive factors, including cytokines (including interleukin-15 (IL-15)), required for the survival and optimal function of tumour-specific T cells[1]. IL-15 belongs to the common γ-chain cytokine family and is important for $CD8^+$ T cell memory formation, mitochondrial metabolism and the expansion and persistence of antigen-experienced T cells[2]. In non-clinical models, IL-15 co-expression in CAR T cells significantly improves their ability to expand, persist and induce complete tumour regression[3,4,14]; however, it is unknown how IL-15 impacts CAR T cell antitumour activity and safety in humans.

Glypican-3 (GPC3) is expressed in a group of solid neoplasms, including hepatocellular carcinoma, the third-most common cause of cancer-related death in the world[5–9]. It is not expressed in non-malignant tissues, making it an attractive immunotherapeutic target[10]. We have previously shown that IL-15 co-expression increases the expansion and antitumour activity of GPC3-expressing CAR T cells (hereafter GPC3 CAR T cells) in non-clinical solid tumour models[15]. To study GPC3 CAR T cells co-expressing IL-15 (15.CAR) in humans, we assessed a total of 24 patients, 12 with CAR T cells and 12 with 15.CAR T cells, in ongoing phase I studies. Here we report safety characteristics and antitumour response rates, establish expansion kinetics in the peripheral blood,

[1]Texas Children's Cancer Center, Department of Pediatrics, Baylor College of Medicine, Houston, TX, USA. [2]Center for Advanced Innate Cell Therapy, Baylor College of Medicine, Houston, TX, USA. [3]Dan L Duncan Comprehensive Cancer Center, Baylor College of Medicine, Houston, TX, USA. [4]Center for Cell and Gene Therapy, Baylor College of Medicine, Houston Methodist Hospital and Texas Children's Hospital, Houston, TX, USA. [5]Department of Immunology and Microbiology, Baylor College of Medicine, Houston, TX, USA. [6]Department of Radiology, Baylor College of Medicine, Houston, TX, USA. [7]Department of Pediatrics, Children's Hospital of Philadelphia and Perelman School of Medicine at the University of Pennsylvania, Philadelphia, PA, USA. [8]Pathology and Laboratory Medicine, Children's Hospital of Philadelphia and Perelman School of Medicine at the University of Pennsylvania, Philadelphia, PA, USA. [9]William A. Brookshire Department of Chemical and Biomolecular Engineering, University of Houston, Houston, TX, USA. [10]Pathology and Immunology Graduate Program, Baylor College of Medicine, Houston, TX, USA. [11]Department of Pathology, Baylor College of Medicine, Houston, TX, USA. [12]Department of Bone Marrow Transplantation and Cellular Therapy, St. Jude Children's Research Hospital, Memphis, TN, USA. [13]Lineberger Comprehensive Cancer Center, University of North Carolina, Chapel Hill, NC, USA. [14]Texas Children's Hospital Liver Tumor Program, Houston, TX, USA. ✉e-mail: heczey@bcm.edu

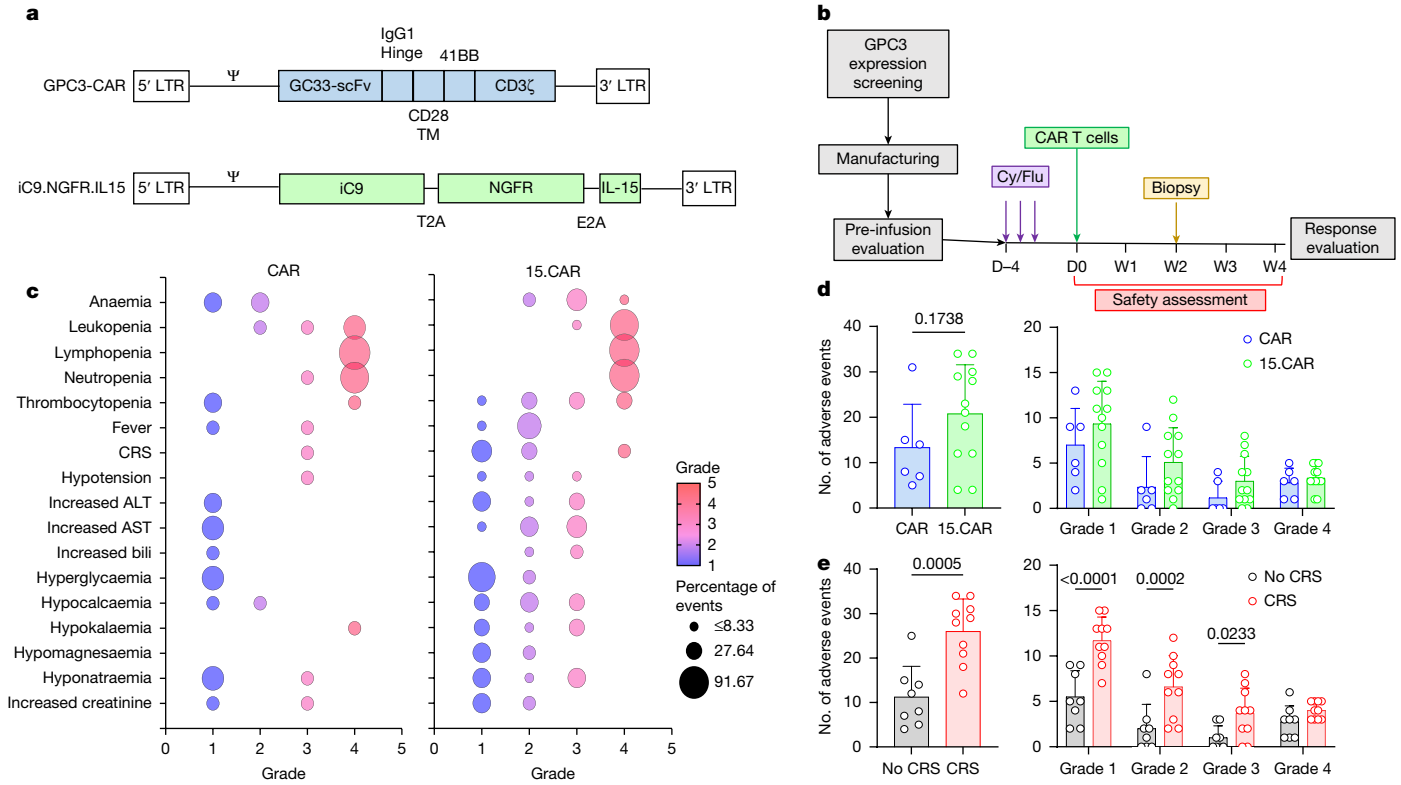

Fig. 1 | Safety characteristics of CAR and 15.CAR infusions. a, Transgene maps of GPC3 CAR and iC9.NGFR.IL-15 constructs used to cotransduce T cells to generate infusion products. TM, transmembrane domain. **b**, Schematic representation of patient enrolment and treatment. **c**, Bubble plots representing frequency of the indicated adverse events for patients infused with CAR (left) and 15.CAR (right). Adverse events were collected from day −4 (D−4) until day +28 (D28) post-infusion, and graded according to Common Terminology Criteria for Adverse Events version 5.0. The colour spectrum corresponds to adverse event grades 1–5, bubble size corresponds to frequencies. **d**, Comparison of frequency of adverse events between CAR ($n = 6$) and 15.CAR ($n = 12$). **e**, Comparison of adverse events between patients with ($n = 10$) and without CRS ($n = 8$), using two-tailed *t*-test and two-way analysis of variance (ANOVA) with Šidák correction, respectively; mean ± s.d. ALT, alanine aminotransferase; AST, aspartate aminotransferase; bili, bilirubin; LTR, long terminal repeat; W1, week 1.

describe trafficking to tumour tissues and determine gene expression changes in CAR and 15.CAR T cells in peripheral blood and within tumours, using single-cell RNA sequencing (scRNA-seq).

15.CAR T cell safety

Immunotherapeutic targeting of GPC3 has previously been established in adults using antibodies, vaccines and CAR T cells[16–18]. We confirmed the absence of GPC3 expression in children using a comprehensive, non-malignant paediatric tissue array[19] and, as part of eligibility before the enrolment of each patient, GPC3 expression in tumour samples was quantified by immunohistochemistry[20] (Extended Data Fig. 1a–c). Patients were enrolled to receive either CAR T cells or 15.CAR T cells (Fig. 1a, Extended Data Fig. 2 and Extended Data Table 1). All patients underwent lymphodepletion with cyclophosphamide and fludarabine, followed by cell infusion and 28 days of monitoring to assess safety (Fig. 1b). Six patients were infused with CAR T cells on dose level (DL)1 at 1×10^7 CAR T cells m^{-2}, and six on DL2 at 3×10^7 m^{-2} (children on NCT02932956, adults on NCT02905188). On both DL1 and DL2, the infusions were safe, no antitumour responses were observed, CAR T cells were detected in peripheral blood and tumour tissues and no significant differences were found in these measures between DLs (Extended Data Fig. 3). Most grade 3–4 adverse events were related to lymphodepletion and are common in patients receiving cell therapy. Next, 12 patients were infused with 15.CAR T cells at 3×10^7 m^{-2} (DL2; children on NCT04377932, adults on NCT05103631). No significant difference was detected in the number of adverse events on DL2 in patients treated with CAR ($n = 6$) versus 15.CAR ($n = 12$) T cells (Fig. 1c,d). However, the incidence of cytokine release syndrome (CRS) requiring treatment with at least immunomodulation (IL-1 or IL-6 inhibition) was increased in the 15.CAR group (relative risk 3.3, 95% confidence interval 1.226–9.723, $P = 0.043$). Adverse events were more common in patients with CRS, with more grade 1, 2 and 3 adverse events being observed in this group, though there was not an increase in number of 4 adverse events (Fig. 1e and Supplementary Table 1). Changes in circulating cytokine levels, including IL-15, were similar in the CAR and 15.CAR cohorts (Extended Data Fig. 4a,b), and patients with CRS had increased concentrations of CCL2, TNF, eotaxin and MIP1β (Extended Data Fig. 4c,d). The inducible caspase 9 (iC9) safety switch was deployed in three patients treated with 15.CAR T cells[21]. The first patient (15.CAR 1) had a prolonged grade 3 CRS event with fever, tachycardia and tachypnoea, and required over 40% O_2 through a high-flow nasal cannula. The second patient (15.CAR 5) had a prolonged grade 2 event with fever, tachycardia and tachypnoea, but less than 40% O_2 requirement. The third patient (15.CAR 9), who had a history of smoking (40 packs per year) and chronic obstructive pulmonary disease, developed fever, tachycardia and hypoxia, which required mechanical ventilation. All three patients received a single intravenous dose of rimiducid, the chemical inducer of dimerization for iC9, after which all three showed rapid improvement in symptoms, effective reduction in circulating 15.CAR T cells and normalization of inflammatory cytokine levels (Extended Data Fig. 4e–g). These results demonstrate that CAR T cell-related toxicities can be quickly resolved if needed in patients who are refractory to IL-1/IL-6 inhibition.

Antitumour responses by 15.CAR T cells

For comparison of antitumour response rates in patients infused with CAR versus 15.CAR T cells, we evaluated changes in pre- and

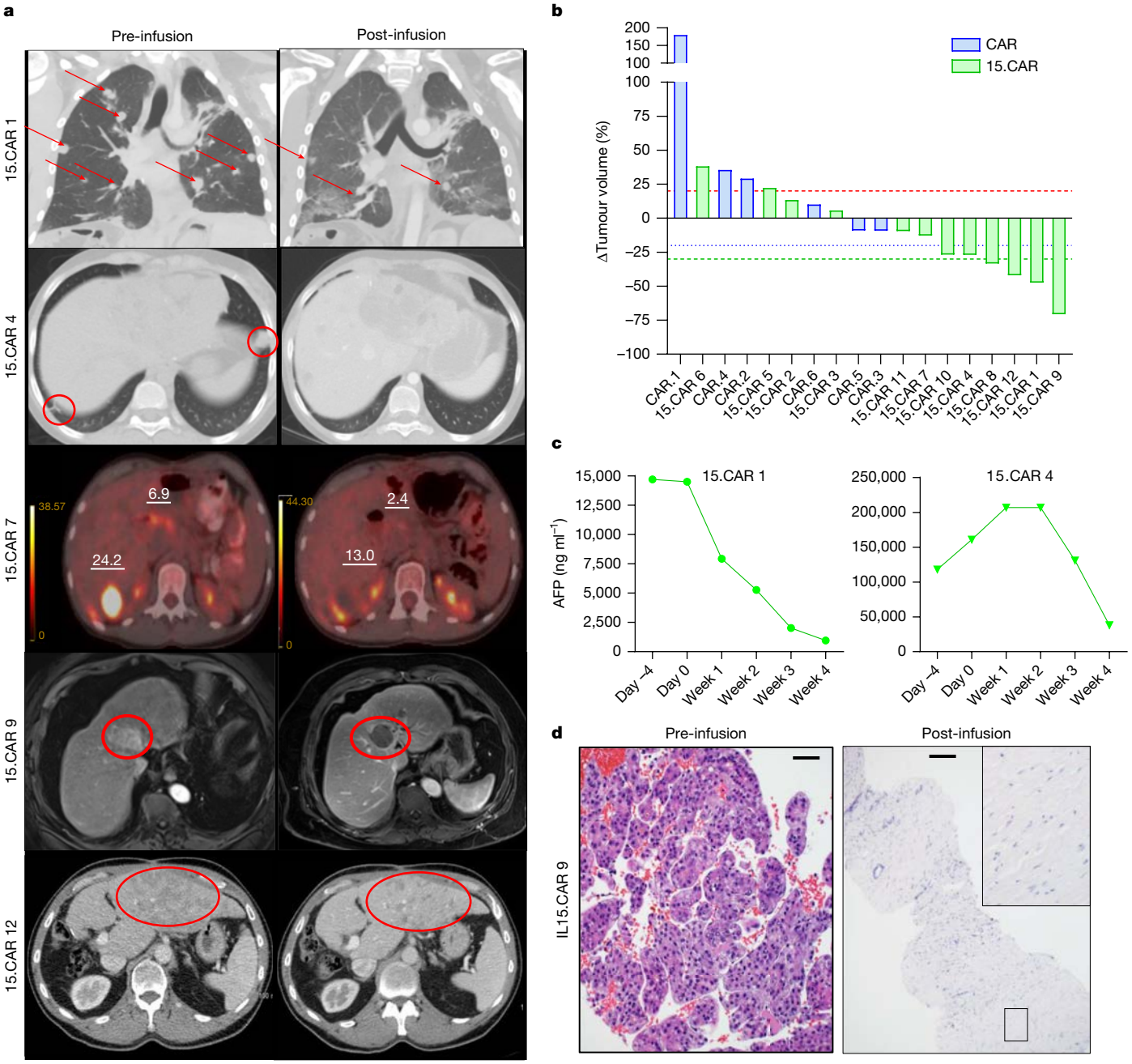

Fig. 2 | 15.GPC3 CAR T cells induce significant antitumour responses in patients. a–**d**, Antitumour responses were determined by comparison of pre- and post-infusion three-dimensional imaging. **a**, Coronal computed tomography (CT) images of chest (15.CAR 1), axial CT chest (no. 15.CAR 4), PET–CT (15.CAR 7), MRI abdomen (15.CAR 9) and axial CT abdomen (15.CAR 12) showing pre- and post-CAR T cell infusion. Red arrows and circles represent tumours. Numbers represent standardized uptake values of tumours in the liver shown by PET. **b**, Waterfall plot representing changes in tumour volumes of patients treated with 3×10^7 m^{-2} CAR or 15.CAR T cells. Red dashed line represents 20% increase, blue dashed line 20% decrease, green dashed line 30% decrease. **c**, Serum AFP concentrations at indicated time points in responders with AFP-secreting neoplasms. **d**, Pre- (left) and post-infusion tumour biopsy (right), assessed with haematoxylin and eosin staining and performed once in the clinical pathology laboratory, showing near-complete necrosis of patient no. 15.CAR 9's liver tumour. Scale bars, 500 µm (pre-infusion), 1,000 µm (post-infusion).

post-infusion three-dimensional imaging and serum α-fetoprotein (AFP) concentrations. Objective responses were not detected in the six patients of the CAR cohort infused at 3×10^7 CAR T cells m^{-2} (DL2); three patients had progressive disease and three had stable disease (SD). By contrast, among the 12 patients infused with 15.CAR T cells on the same dose level, four had progressive disease, four had SD and four had a partial response according to Response Evaluation Criteria in Solid Tumurs (RECIST) criteria[22] (Extended Data Table 1). Among those with SD, patient 15.CAR 4 and 15.CAR 10 had over 26% reduction in tumour burden. Patient 15.CAR 7 had a reduction of approximately 12.8% and a significant decrease in positron emission tomography (PET) avidity of residual masses, providing evidence of antitumour activity even if it did not meet RECIST criteria (Fig. 2a,b and Extended Data Fig. 5a). Two of the responding patients had AFP-secreting tumours, and both showed significant reduction in AFP levels (Fig. 2c and Extended Data Fig. 5b). When comparing serum cytokine profiles, eotaxin and CCL22 concentrations were elevated in responders (Extended Data Fig. 5c,d). No difference was detected in the GPC3 expression of pre-enrolment tumours between responder and non-responder patients (Extended Data Fig. 5e). In patient 15.CAR 9, magnetic resonance imaging (MRI) of the

patient's liver tumour suggested complete necrosis, and image-guided sampling of the lesions confirmed near-complete necrosis of the primary liver tumour (Fig. 2d). Collectively, patients treated with 15.CAR T cells had a disease control rate (SD and progressive disease) of 66.7% (8 of 12) and an objective response rate of 33.3% (4 of 12).

Multiomic characteristics of CAR T cells

Specific transcriptomic and cell surface phenotypic characteristics of CAR T cell infusion products have been associated with differences in clinical outcomes[23,24]. For comparison of the baseline gene expression profile of CAR and 15.CAR T cells, we analysed a total of 36,722 cells by scRNA-seq. We found that CAR and 15.CAR T cell products had differential enrichment of gene expression across 12 unique cell clusters (C0–C11; Fig. 3a–c). We identified 3,285 differentially expressed genes in 15.CAR T versus CAR T cell products, including increased expression of *CD8A/B*, *ZNF683* (encoding HOBIT) and genes related to cytolytic activity (*GZM* genes, *PRF1* and *NKG7*), as well as downregulation of costimulatory receptors (*TNFRSF4*, *TNFRSSF9* and *TNFRSF18*) and *TCF7* (Fig. 3d and Extended Data Fig. 6a). In addition, IL-15 co-expression induced lower glycolytic and higher oxidative phosphorylation (OXPHOS) signatures in products (Extended Data Fig. 6b). At the protein level, compared with CAR T cell products, 15.CAR T cells were enriched for the CD8 subset and showed a significantly lower frequency of central memory cells, with a corresponding increase in effector memory and effector subsets (Fig. 3e). Compared with CAR T products, 15.CAR products had a similar frequency of $PD1^+$ and $TIM3^+$ cells but a higher frequency of $LAG3^+$ cells (Extended Data Fig. 6c). Double-negative CD39/CD69 cells, which are associated with improved antitumour responses in patients treated with tumour-infiltrating lymphocytes (TILs)[25], had similar frequency in both products (Extended Data Fig. 6c). Because T cells differentiate from naive into memory and then terminal effector cells, their ability to kill and produce cytokines increases. Consistent with gene expression and phenotype results, 15.CAR T cells showed significantly higher cytolytic activity and were more polyfunctional[26] than CAR T cells, primarily due to their producing more effector cytokines (Fig. 3f,g and Extended Data Fig. 6d,e). Sustained antigen-dependent proliferation is necessary for CAR T cells to maintain or increase the pool of tumour-specific effectors and reduce tumour masses with large numbers of neoplastic cells. 15.CAR T cells expanded significantly more than CAR T cells in peripheral blood, and this difference was also significant in responders versus non-responders in the 15.CAR cohort (Fig. 3i–k and Extended Data Fig. 7a–c). We did not detect differences in the frequencies of invariant natural killer T cell (iNKT) or NK cell subsets in peripheral blood of CAR- versus 15.CAR-treated patient groups (Extended Data Fig. 7d). Although the frequency of tumour-infiltrating CAR and 15.CAR T cells was similar, these results may have been biased in some patients infused with 15.CAR T cells due to activation of the iC9 safety switch and resultant reduction in cell numbers at the time of biopsy (Extended Data Fig. 7d,e). Collectively, these results show that 15.CAR T cell products were more ready pre-infusion to execute effector function and were able to expand better in patients than CAR T cells. These factors probably contributed to the overall more potent antitumour activity.

Evolution of 15.CAR T cells in patients

The transcriptomic evolution of CAR T cells in peripheral blood and in the TME of patients with solid tumours is poorly understood, and gene expression profiles associated with increased expansion and superior antitumour responses of infused CAR T cells remain to be established. We used scRNA-seq to compare the gene expression profiles of pre-infusion products with cells collected from peripheral blood (35,906 cells) and tumour biopsies (10,382 cells) 2–3 weeks post-infusion. Both CAR and 15.CAR T cells collected from peripheral blood demonstrated upregulation of genes and gene sets associated with NK-like differentiation, cytotoxic effector activity[27] and exhaustion[28]. In addition, genes associated with less differentiated memory cells and cytokine signalling, as well as corresponding gene sets (that is, chromatin remodelling and mitotic spindle organization)[29], were downregulated in both groups (Extended Data Fig. 8a,b). These observations suggest that both CAR and 15.CAR T cells were exposed to tumour cells and had initiated effector differentiation leading to decreased proliferative capacity. However, the gene expression profiles of CAR T and 15.CAR T cells in peripheral blood diverged for genes involved in adhesion/effector function, IL-15 signalling, cellular metabolism, NF-κB signalling, innate antiviral response and survival[30,31] (Extended Data Fig. 8a,c). Because T cells captured from peripheral blood are different from those in tumour tissues, we also evaluated the gene expression profile of adoptively transferred cells isolated from tumours. We could not capture sufficient numbers of CAR T cells for scRNA-seq analysis from tumour biopsies of patients in the CAR cohort, and therefore it was not possible to compare the CAR and 15.CAR cohorts. By contrast, tumour-infiltrating 15.CAR T cells were captured effectively, and we compared gene expression in responders with evidence of antitumour activity (at least 20% reduction in tumour size) versus non-responders. Ten clusters of tumour-infiltrating 15.CAR T cells were identified; responders were enriched in cluster 0 (Fig. 4a–c). To determine the evolution of 15.CAR T cells post-infusion, we compared their gene expression change with baseline (pre-infusion product). For both responders and non-responders, genes associated with cytotoxicity, NK-like transition, terminal effector differentiation and exhaustion were upregulated. In parallel, genes related to less differentiated naive and memory subsets were downregulated in both groups (Fig. 4d). Gene Ontology analyses showed that both responders and non-responders were enriched for expression of programs related to membrane-initiated signalling, NK immunity, cytotoxic response and downregulation of programs related to ATP generation and replication (Fig. 4e and Supplementary Table 3), demonstrating activation and effector differentiation in the TME while losing proliferative capacity. However, in contrast to cells from non-responders, 15.CAR T cells from responders showed upregulation of AP1 family members *FOS*, *FOSB*, *JUN*, *JUNB* and *JUND*, regulators of T cell survival, and of genes associated with type I interferon (T1IFN) signalling as well as repression of genes in the SWI/SNF chromosome remodelling complex[32,33] (Fig. 4f and Extended Data Fig. 8d). The majority of CAR^+ TILs were $CD8^+$, and no difference was detected between CAR TIL subsets including iNKTs or NK cells in responder versus non-responder patients (Extended Data Fig. 8e,f). To assess the bystander effect associated with response, we evaluated the gene expression profile of these cells and identified increases in T1IFN, OXPHOS and cytolytic signatures in CAR TILs from responder versus non-responder patients (Extended Data Fig. 9a,b). Using variable-diversity joining sequences of transcription-coupled repairs (TCRs), we detected T cell clones expanding from the product in peripheral blood and biopsies (Extended Data Fig. 9c) and, to further examine bystander T effect in the TME, we assessed whether there was evidence of intratumoural expansion of either CAR^+ or CAR^- T cells by comparing the number of T cells with the same TCR in responders versus non-responders[34]. Although no difference was detected in CAR^+ TILs compared with non-responders, a significant increase was detected in the intratumoural expansion of CAR^- TILs in responders (Extended Data Fig. 9d). These changes demonstrate robust evolution in the TME and identify genes and programs associated with responses in patients treated with 15.CAR T cells.

Discussion

CAR T cells induce significant antitumour responses in patients with haematologic malignancies, and hold tremendous promise in regard to helping patients with solid tumours. Recent clinical studies have demonstrated higher frequencies of antitumour responses in patients

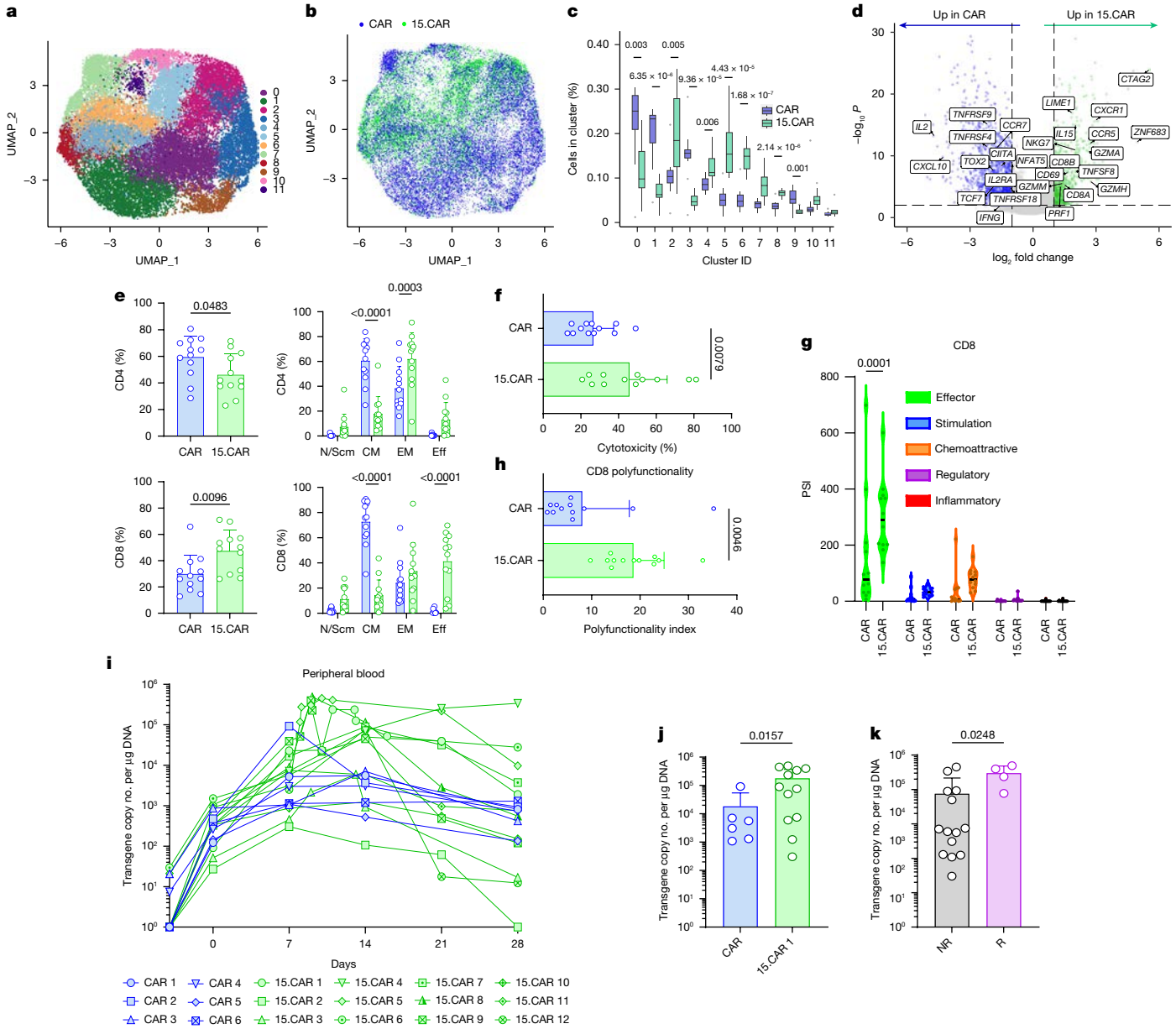

Fig. 3 | Comparison of pre-infusion products and expansion in patients infused with CAR or 15.CAR T cells. a–**k**, Products were first assessed with scRNA-seq. **a**, Uniform manifold approximation and projection (UMAP) identified unique T cell clusters in integrated CAR and 15.CAR pre-infusion products. **b**,**c**, Differential representation of CAR ($n = 12$) versus 15.CAR ($n = 12$) T cells in clusters shown in UMAP projection (**b**), and proportions of each cluster (**c**). Centre line denotes median, box limits first and third quartiles, whiskers 1.5× interquartile range, dots outliers. Percentages of cells in clusters were compared using unpaired two-tailed Student's *t*-test. Shown are adjusted *P* values using Benjamini–Hochberg correction. **d**, Differentially expressed genes in CAR ($n = 12$) versus 15.CAR ($n = 12$) products. **e**, Frequencies of CD4/8 and effector/memory subsets in CAR ($n = 12$) versus 15.CAR ($n = 12$) products, as demonstrated by flow cytometry. Data represent mean ± s.d. Two-tailed, unpaired *t*-test and two-way ANOVA with Šídák correction, respectively. N/Scm, naive, stem cell memory; CM, central memory; EM, effector memory; Eff, effector. **f**, Cytotoxicity of CAR ($n = 12$) versus 15.CAR ($n = 12$) products, as measured by ^{51}Cr release assay. Two-tailed, unpaired *t*-test, data represented as mean ± s.d. **g**, Polyfunctionality strength index (PSI) comparing CAR ($n = 12$) versus 15.CAR ($n = 12$) T cell product cytokine production by IsoPlexis. Two-way ANOVA with Šídák correction. **h**, Differentially expressed cytokines in CD8 subsets of CAR ($n = 12$) and 15.CAR ($n = 12$) T cell products. Two-tailed, unpaired *t*-test, data represented as mean ± s.d. **i**, Peripheral blood CAR T cell frequencies, quantified by quantitative PCR at the indicated time points for each patient. **j**, Comparison of peak expansion on DL 2 of CAR ($n = 6$) versus 15.CAR ($n = 12$) T cells post-infusion. Two-tailed, unpaired *t*-test. Data represented as mean ± s.d. **k**, Comparison of expansion of cells in responders (R, $n = 4$) versus non-responders (NR, $n = 14$). Two-tailed, unpaired Mann–Whitney test, data represented as mean ± s.d.

with low-burden neuroblastoma[35], and in brain tumours treated with repeat infusions[36].

In this first-in-human assessment, we evaluated the impact of transgenic IL-15 expression in GPC3 CAR T cells in patients with GPC3-positive solid cancers. Systemic administration of IL-15 has been associated with significant toxicities due to high serum concentrations[37]. In this study, although CRS was more common in 15.CAR- versus CAR T cell-treated patients, IL-15 serum concentrations were not higher, suggesting that these events were probably due to marked T cell activation. CRS-related side effects were effectively controlled through IL-6/IL-1 blockade in most patients. The iC9 safety switch has been proven to effectively eliminate alloreactive T cells in patients[38]. Here we provide evidence that iC9 mediates rapid elimination of CRS induced by CAR T cells that is resistant to other interventions.

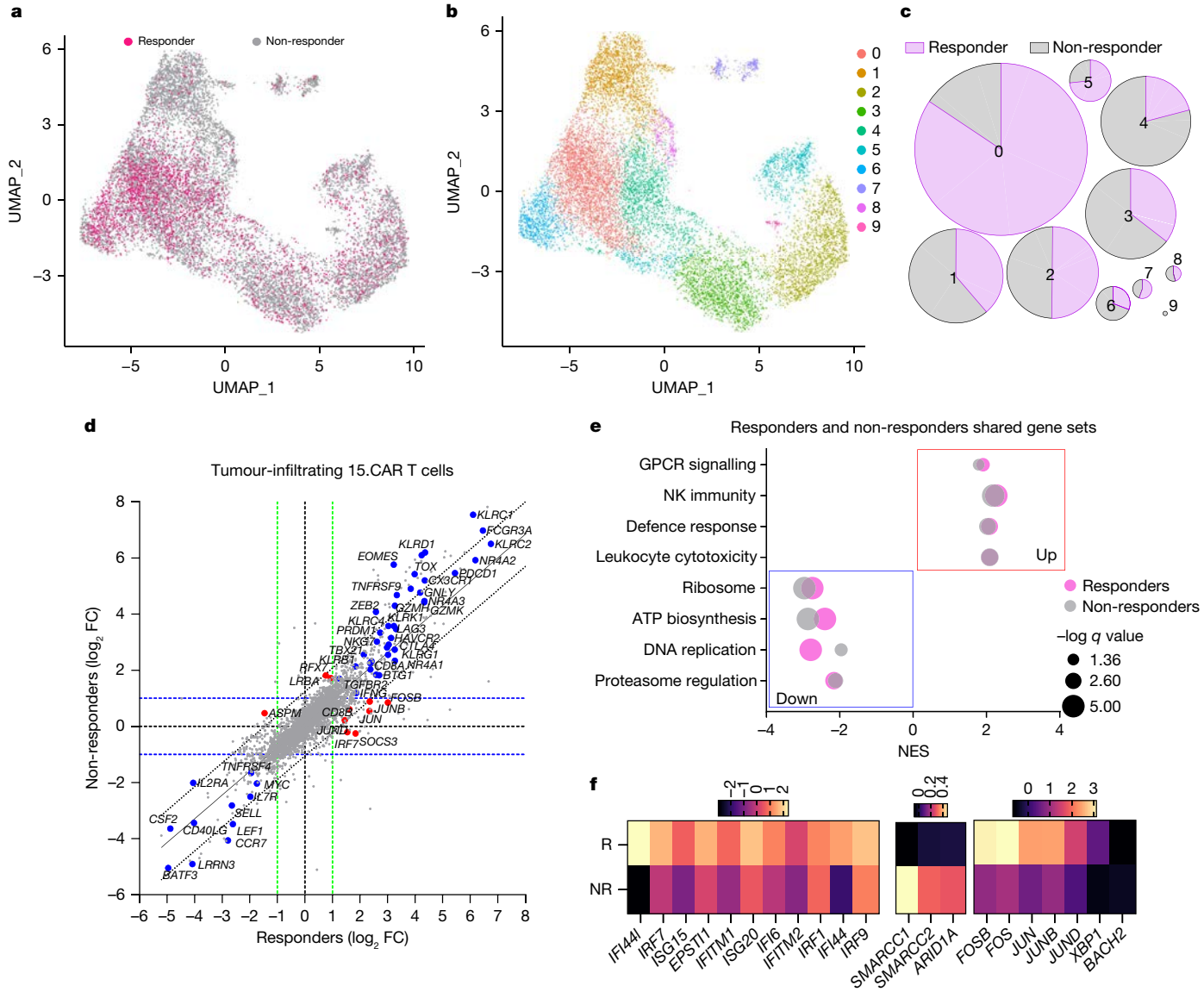

Fig. 4 | Comparison of the single-cell gene expression profile of tumour-infiltrating 15.CAR T cells post-infusion in responders versus non-responders. **a**–**f**, The transcriptomic profile of infusion products and tumour-infiltrating 15.CAR T cells was interrogated using scRNA-seq. Differentially expressed genes (DEGs) for the indicated groups were determined by comparison of the product with tumour-derived 15.CAR T cells. **a**, UMAP projection of tumour-infiltrating 15.CAR T cells from responders and non-responders. **b**, Unsupervised clustering of tumour-infiltrating CAR T cells of responders and non-responders from the 15.CAR cohort. **c**, Differences in cluster proportions for the indicated groups. **d**, DEG comparison (product versus tumour-infiltrating 15.CAR T cells) in responders (*x* axis) versus non-responders (*y* axis) from the 15.CAR cohort (linear regression). **e**, Gene sets enriched in tumour-infiltrating 15.CAR T cells. **f**, Heatmap representing genes with the greatest differences in change from baseline in responders (R) versus non-responders (NR) in 15.CAR T cells. FC, fold change; NES, normalized enrichment score.

Antitumour responses were more frequent in patients treated with 15.CAR T cells compared with those treated with CAR T cells, and in comparison with patients treated on a previous phase I study of T cells expressing a third-generation GPC3 CAR[17]. The antitumour activity of 15.CAR T cells may have been underestimated in our study, because we have not yet evaluated higher doses: dose escalation is ongoing in our phase I trial, and repeat infusion schedules may also be considered.

Previous preclinical reports raised concerns about malignant transformation of T cells engineered with IL-15 (ref. 39). Our study provides evidence for the absence of IL-15-mediated transformation in T cells manufactured from mature peripheral blood mononuclear cells (PBMCs). In fact, T cells expressing the iC9.IL-15 construct without GPC3 CAR were not detectable shortly after infusion, suggesting that in vivo expansion of these cells remains antigen dependent. Unexpectedly, elimination of iC9.IL-15-expressing cells reduced populations of both CAR-positive and CAR/IL-15-dual-positive circulating populations, raising the possibility that paracrine or cross-presentation of IL-15 promotes CAR T cell survival. Identifying the specific dose of rimiducid to eliminate side effects without significant effect on CAR T cell persistence is a focus of active investigation in our group.

IL-15 maintains $CD8^+$ T cells, increases OXPHOS and promotes memory formation[2]. 15.CAR T cells contained a higher proportion of $CD8^+$ cells and had higher OXPHOS gene expression signatures but showed a more effector-differentiated transcriptomic and cell surface phenotype, with higher ex vivo cytolytic activity and increase in polyfunctionality. Because the products were manufactured under identical conditions, including supplementation with IL-7 and IL-15 (ref. 40), the cotransduction procedure may have contributed to these differences. Interestingly, despite increased effector differentiation,

the expansion of 15.CAR T cells was significantly higher compared with that of CAR T cells. Collectively, these data demonstrate that, in CAR T cell products of patients, the co-expression of IL-15 induces a mixed program of effector differentiation with increased OXPHOS gene expression signature and enhanced proliferative capacity associated with improved antitumour activity.

Understanding the evolution of gene expression programs in CAR T cells post-infusion should provide critical insights into the identification of master regulator genes and gene sets associated with cell survival and sustained effector function. CAR T cells co-expressing *JUN* had increased antitumour activity in non-clinical models[41], and our results demonstrate the importance of FOS and JUN subfamily members, because these genes were significantly upregulated in tumour-infiltrating 15.CAR T cells in responders. Previously, ex vivo screening methods demonstrated that decreasing the function of the SWI/SNF chromosomal remodelling complex can enhance CAR T cell antitumour function[33]. Consistent with this observation, we found that *ARID1A* expression was repressed in tumour-infiltrating 15.CAR T cells of responders. *IRF7* expression has been shown to be necessary for CAR T cell survival[42], but results from non-clinical models have been inconclusive as to whether IRF7 is associated with exhaustion or antitumour function[42–44]. Our results from tumour-infiltrating 15.CAR T cells provide evidence that *IRF7* and associated factors related to T1IFN signalling indeed have a role in supporting antitumour function in the human TME. The data also demonstrate the effects on bystander T cells, including specific gene expression signature changes and intratumour expansion associated with antitumour responses. The establishment of whether these gene expression changes are drivers of, or are simply associated with, clinical responses will be a focus of future ex vivo gain- and loss-of-function experiments.

In conclusion, single infusions of 15.CAR T cells are safe and mediate increased antitumour response rates and expansion in patients with solid tumours. Furthermore, increased expression of *FOS*/*JUN* and T1IFN pathway-related genes, as well as downregulation of SWI/SNF activity in intratumoural 15.CAR T cells, were associated with response to therapy.

Online content

Any methods, additional references, Nature Portfolio reporting summaries, source data, extended data, supplementary information, acknowledgements, peer review information; details of author contributions and competing interests; and statements of data and code availability are available at https://doi.org/10.1038/s41586-024-08261-8.

1. Mlecnik, B. et al. Functional network pipeline reveals genetic determinants associated with in situ lymphocyte proliferation and survival of cancer patients. *Sci. Transl. Med.* **6**, 228ra237 (2014).
2. Pilipow, K. et al. IL15 and T-cell stemness in T-cell-based cancer immunotherapy. *Cancer Res.* **75**, 5187–5193 (2015).
3. Brentjens, R. J. et al. Eradication of systemic B-cell tumors by genetically targeted human T lymphocytes co-stimulated by CD80 and interleukin-15. *Nat. Med.* **9**, 279–286 (2003).
4. Hoyos, V. et al. Engineering CD19-specific T lymphocytes with interleukin-15 and a suicide gene to enhance their anti-lymphoma/leukemia effects and safety. *Leukemia* **24**, 1160–1170 (2010).
5. Chan, E. S. et al. Immunohistochemical expression of glypican-3 in pediatric tumors: an analysis of 414 cases. *Pediatr. Dev. Pathol.* **16**, 272–277 (2013).
6. Haruyama, Y. & Kataoka, H. Glypican-3 is a prognostic factor and an immunotherapeutic target in hepatocellular carcinoma. *World J. Gastroenterol.* **22**, 275–283 (2016).
7. Tretiakova, M. et al. Glypican 3 overexpression in primary and metastatic Wilms tumors. *Virchows Arch.* **466**, 67–76 (2015).
8. Kohashi, K. et al. Glypican 3 expression in tumors with loss of SMARCB1/INI1 protein expression. *Hum. Pathol.* **44**, 526–533 (2013).
9. Zynger, D. L., Dimov, N. D., Luan, C., Teh, B. T. & Yang, X. J. Glypican 3: a novel marker in testicular germ cell tumors. *Am. J. Surg. Pathol.* **30**, 1570–1575 (2006).
10. Ho, M. & Kim, H. Glypican-3: a new target for cancer immunotherapy. *Eur. J. Cancer* **47**, 333–338 (2011).
11. Maude, S. L. et al. Tisagenlecleucel in children and young adults with B-cell lymphoblastic leukemia. *N. Engl. J. Med.* **378**, 439–448 (2018).
12. Park, J. H. et al. Long-term follow-up of CD19 CAR therapy in acute lymphoblastic leukemia. *N. Engl. J. Med.* **378**, 449–459 (2018).
13. Yong, C. S. M. et al. CAR T-cell therapy of solid tumors. *Immunol. Cell Biol.* **95**, 356–363 (2017).
14. Chen, Y. et al. Eradication of neuroblastoma by T cells redirected with an optimized GD2-specific chimeric antigen receptor and interleukin-15. *Clin. Cancer Res.* **25**, 2915–2924 (2019).
15. Batra, S. A. et al. Glypican-3-specific CAR T cells coexpressing IL15 and IL21 have superior expansion and antitumor activity against hepatocellular carcinoma. *Cancer Immunol. Res.* **8**, 309–320 (2020).
16. Ishiguro, T. et al. Anti-glypican 3 antibody as a potential antitumor agent for human liver cancer. *Cancer Res.* **68**, 9832–9838 (2008).
17. Shi, D. et al. Chimeric antigen receptor-glypican-3 T-cell therapy for advanced hepatocellular carcinoma: results of Phase I trials. *Clin. Cancer Res.* **26**, 3979–3989 (2020).
18. Sawada, Y. et al. Phase II study of the GPC3-derived peptide vaccine as an adjuvant therapy for hepatocellular carcinoma patients. *Oncoimmunology* **5**, e1129483 (2016).
19. Bosse, K. R. et al. Identification of GPC2 as an oncoprotein and candidate immunotherapeutic target in high-risk neuroblastoma. *Cancer Cell* **32**, 295–309 (2017).
20. Zhu, A. X. et al. First-in-man phase I study of GC33, a novel recombinant humanized antibody against glypican-3, in patients with advanced hepatocellular carcinoma. *Clin. Cancer Res.* **19**, 920–928 (2013).
21. Di Stasi, A. et al. Inducible apoptosis as a safety switch for adoptive cell therapy. *N. Engl. J. Med.* **365**, 1673–1683 (2011).
22. Eisenhauer, E. A. et al. New response evaluation criteria in solid tumours: revised RECIST guideline (version 1.1). *Eur. J. Cancer* **45**, 228–247 (2009).
23. Deng, Q. et al. Characteristics of anti-CD19 CAR T cell infusion products associated with efficacy and toxicity in patients with large B cell lymphomas. *Nat. Med.* **26**, 1878–1887 (2020).
24. Gardner, R. et al. Starting T cell and cell product phenotype are associated with durable remission of leukemia following CD19 CAR-T cell immunotherapy. *Blood* **132**, 4022–4022 (2018).
25. Krishna, S. et al. Stem-like CD8 T cells mediate response of adoptive cell immunotherapy against human cancer. *Science* **370**, 1328–1334 (2020).
26. Rossi, J. et al. Preinfusion polyfunctional anti-CD19 chimeric antigen receptor T cells are associated with clinical outcomes in NHL. *Blood* **132**, 804–814 (2018).
27. Good, C. R. et al. An NK-like CAR T cell transition in CAR T cell dysfunction. *Cell* **184**, 6081–6100 (2021).
28. Seo, H. et al. TOX and TOX2 transcription factors cooperate with NR4A transcription factors to impose CD8(+) T cell exhaustion. *Proc. Natl Acad. Sci. USA* **116**, 12410–12415 (2019).
29. Murphy, K., Travers, P., Walport, M. & Janeway, C. *Janeway's Immunobiology* (Garland Science, 2012).
30. Mahuron, K. M. et al. Layilin augments integrin activation to promote antitumor immunity. *J. Exp. Med.* **217**, e20192080 (2020).
31. Wang, C., Lin, G. H., McPherson, A. J. & Watts, T. H. Immune regulation by 4-1BB and 4-1BBL: complexities and challenges. *Immunol. Rev.* **229**, 192–215 (2009).
32. Murphy, K. M. & Weaver, C. *Janeway's Immunobiology: Tenth International Student Edition with Registration Card* (W.W. Norton, 2022).
33. Belk, J. A. et al. Genome-wide CRISPR screens of T cell exhaustion identify chromatin remodeling factors that limit T cell persistence. *Cancer Cell* **40**, 768–786 (2022).
34. Upadhye, A. et al. Intra-tumoral T cells in pediatric brain tumors display clonal expansion and effector properties. *Nat. Cancer* **5**, 791–807 (2024).
35. Del Bufalo, F. et al. GD2-CART01 for relapsed or refractory high-risk neuroblastoma. *N. Engl. J. Med.* **388**, 1284–1295 (2023).
36. Majzner, R. G. et al. GD2-CAR T cell therapy for H3K27M-mutated diffuse midline gliomas. *Nature* **603**, 934–941 (2022).
37. Conlon, K. C. et al. Redistribution, hyperproliferation, activation of natural killer cells and CD8 T cells, and cytokine production during first-in-human clinical trial of recombinant human interleukin-15 in patients with cancer. *J. Clin. Oncol.* **33**, 74–82 (2015).
38. Straathof, K. C. et al. An inducible caspase 9 safety switch for T-cell therapy. *Blood* **105**, 4247–4254 (2005).
39. Fehniger, T. A. et al. Fatal leukemia in interleukin 15 transgenic mice follows early expansions in natural killer and memory phenotype $CD8^+$ T cells. *J. Exp. Med.* **193**, 219–231 (2001).
40. Xu, Y. et al. Closely related T-memory stem cells correlate with in vivo expansion of CAR. CD19-T cells and are preserved by IL-7 and IL-15. *Blood* **123**, 3750–3759 (2014).
41. Lynn, R. C. et al. c-Jun overexpression in CAR T cells induces exhaustion resistance. *Nature* **576**, 293–300 (2019).
42. Zhao, Z. et al. Structural design of engineered costimulation determines tumor rejection kinetics and persistence of CAR T cells. *Cancer Cell* **28**, 415–428 (2015).
43. Jung, I.-Y. et al. Type I interferon signaling via the EGR2 transcriptional regulator potentiates CAR T cell-intrinsic dysfunction. *Cancer Discov.* **13**, 1636–1655 (2023).
44. Lukhele, S. et al. The transcription factor IRF2 drives interferon-mediated CD8(+) T cell exhaustion to restrict anti-tumor immunity. *Immunity* **55**, 2369–2385 (2022).

Methods

Clinical study design and regulatory approvals

We conducted four phase I clinical trials evaluating autologous T cells expressing a second-generation, GPC3-specific chimeric antigen receptor incorporating the 41BB costimulatory endodomain[45], two of which also co-express the cytokine IL-15 to treat both paediatric (GAP, NCT02932956; AGAR, NCT04377932) and adult patients (GLYCAR, NCT02905188; CATCH, NCT05103631) with relapsed and/or refractory liver tumours. All patients were included in safety analysis. All trials were registered at clinicaltrials.gov before the start of enrolment. All patients received lymphodepletion with cyclophosphamide (500 mg m^{-2} per dose) and fludarabine (30 mg m^{-2} per dose) on days −4, −3 and −2, followed by infusion of GPC3 CAR T cells on D0–2 on two dose levels (DL1 at 1×10^7 CAR^+ T cells m^{-2} and DL2 at 3×10^7 CAR^+ T cells m^{-2}). Dose escalation followed the standard 3 + 3 design for the GPC3 CAR T cell trials, and the Bayesian optimal interval design for 15.GPC3 CAR T cell trials. The study objectives were as follows. The primary aims were to (1) determine the safety of escalating doses of GPC3 CAR T cells, and (2) determine the recommended phase II dose of GPC3 CAR T cells in treating patients with GPC3-positive solid tumours following lymphodepleting chemotherapy. The secondary objectives were to (1) assess the antitumour effect of the infused GPC3-specific CAR T cells in patients with GPC3-positive solid tumours, and (2) assess the in vivo persistence, phenotype and functional activity of infused GPC3 CAR T cells in children with GPC3-positive solid tumours. History and physical examination, along with laboratory testing, were performed on D−4 and D0 and at weeks 1, 2 and 4 post-infusion for all patients. Adverse events were collected from the start of lymphodepletion (D−4) until D28 post-infusion, and are described according to the Common Terminology Criteria for Adverse Events version 5.0. Dose-limiting toxicities were defined as any of the following that might be considered at least potentially related to the study cellular products: (1) any grade 5 event; (2) non-haematologic dose-limiting toxicity (any grade 3 or 4 non-haematologic toxicity that fails to return to grade 2 within 72 h); (3) grade 2–4 allergic reaction to CAR T cell infusion; (4) grade 4 haematologic toxicity that persists for 28 days or longer; (5) grade 3 CRS infusion reactions and neurologic toxicity (if they fail to return to grade 1 within 7 days); and (6) grade 4 CRS and neurologic toxicities. Clinical response assessment was carried out by standard three-dimensional imaging, using CT of the chest and CT or MRI of the abdomen, performed within 2 weeks before GPC3 CAR T cell infusion and again at 4 weeks (range 4–8 weeks). Antitumour response rate was defined by RECIST criteria as previously described[22].

Patient eligibility and logistics

The studies were conducted in two phases: procurement and treatment.

Procurement eligibility. This was determined by (1) relapsed or refractory GPC3-positive solid tumours; (2) age 1–18 years; (3) Lansky or Karnofsky score above 60%; (4) life expectancy above 16 weeks; (5) Child–Turcotte–Pugh score 7 or less (for patients with hepatocellular carcinoma only); and (6) informed consent explained to, understood by and signed by patient and/or guardian.

Exclusion criteria for procurement. These were determined by (1) either history of hypersensitivity reactions to murine protein-containing products or the presence of human anti-mouse antibody before enrolment (only patients who had received previous therapy with murine antibodies); (2) history of organ transplantation; (3) known human immunodeficiency virus positivity; and (4) severe previous toxicity from cyclophosphamide or fludarabine.

Treatment eligibility. In addition to the criteria included for procurement, this was determined by the following: (1) Barcelona Clinic Liver Cancer Stage A, B or C (for patients with hepatocellular carcinoma only); (2) life expectancy of at least 12 weeks; (3) Child–Turcotte–Pugh score 7 or less (for patients with hepatocellular carcinoma only); (4) creatinine clearance, as estimated by Cockcroft–Gault or Schwartz, 60 ml min^{-1} or above; (5) serum AST below five times the upper limit of normal; (6) total bilirubin three times or less the upper limit of normal for age; (7) International Normalized Ratio 1.7 or below (for patients with hepatocellular carcinoma only); (8) absolute neutrophil count above 500 μl^{-1}; (9) platelet count above 25,000 μl^{-1} (can be transfused); (10) haemoglobin 7.0 g dl^{-1} or above (can be transfused); (11) pulse oximetry over 90% on room air; (12) refractory or relapsed disease following treatment with upfront therapy and at least one salvage treatment cycle; (13) recovery from acute toxic effects of all previous chemotherapy and investigational agents before entering this study; and (14) birth control for 3 months following T cell infusion in sexually active patients.

Exclusion criteria for treatment. In addition to the exclusion criteria detailed above for procurement, the following were applied: (1) pregnancy or lactation; (2) uncontrolled infection; (3) systemic steroid treatment (0.5 mg of prednisone equivalent kg^{-1} d^{-1}); (4) known human immunodeficiency virus positivity; and (5) active bacterial, fungal or viral infection (except hepatitis B or C virus infections).

The clinical trials and corresponding protocols were reviewed and approved by the Protocol Review Committee, the Institutional Biosafety Committee and the Institutional Review Board at Baylor College of Medicine and the US Food and Drug Administration. Children were enrolled at the Texas Children's Hospital, and adults were treated at Houston Methodist Hospital by members of the Center for Cell and Gene Therapy of Baylor College of Medicine, Houston, Texas, in accordance with Declaration of Helsinki principles. All participants and/or legal guardians provided written informed consent/assent before enrolment on the studies.

Patients with at least SD were eligible for reinfusion if meeting all treatment eligibility criteria. Patient nos. DL1.CAR3, 15.CAR4, 15.CAR7, 15.CAR8 and 15.CAR12 received a second infusion.

Clinical-grade vector production

Both vectors (GPC3.CAR.41BBζ and iC9.NGFR.IL-15) included a standard replication incompetent retrovirus produced from the PG13 packaging producer cell line, which provides Gag-Pol and GALV env in *trans*. The vector genome for each was derived from the SFG backbone, a Moloney-based splicing retroviral vector that lacks all coding for env and most of the Gag-Pol gene, except for the packaging sequence. The vector was further modified by the introduction of base pair substitutions at positions 413, 430 and 635 of the Mo-MuLV sequence, to prevent translation of any portion of the remaining gag sequence. For GPC3.CAR.41BBζ, a codon-optimized minigene was synthesized by GeneArt (Thermo Fisher Scientific) encoding a human immunoglobulin heavy-chain leader peptide and the GPC3-specific single-chain variable fragment GC33. The minigene was subcloned in frame into a retroviral vector containing an expression cassette encoding an IgG1 short hinge, a CD28 transmembrane domain (CD28TM) and 41BB.ζ signalling domains[45]. Transgene integration was confirmed with sequencing, and the producer cell clone was validated under good manufacturing practice guidelines. The final viral supplement was stored at −80 °C and tested before release for clinical testing. For iC9.NGFR.IL-15, a codon-optimized minigene was synthesized by GeneArt, including one T2A-like sequence encoding a 20 amino acid peptide from *Thosea asigna* insect virus (RAEGRGSLLTCGDVEENPGP) and one E2A-like sequence encoding a 20 amino acid peptide from *Equine rhinitis* A virus (RAQCTNYALLKLAGDVESNPGP). These connect iC9, the truncated NGFR gene coding the extracellular and transmembrane domain and the human IL-15 gene. The expression cassette was cloned into the SFG retroviral vector backbone.

CAR T cell manufacture

GPC3 CAR T cells for both protocols were generated using PBMCs from patients first stimulated with CD3 and CD28 monoclonal antibodies (Miltenyi Biotec) in the presence of recombinant human IL-7 (10 ng ml^{-1}) and IL-15 (5 ng ml^{-1}, both from R&D Systems) on D1, and transduced with retroviral particles encoding the GPC3 CAR construct in 24-well, RetroNectin-coated plates (Takara Bio) on D3. Next, T cells were washed and replated on D5, expanded and tested, followed by cryopreservation on D8. 15.GPC3 CAR T cells were also generated using PBMCs stimulated with CD3 and CD28 monoclonal antibodies in the presence of recombinant human IL-7 and IL-15 on D1. They were then transduced with retroviral particles encoding the iC9.NGFR.IL-15 construct in RetroNectin-coated plates on D3, resuspended and transduced with retroviral particles encoding the GPC3 CAR construct on D4.

Immunophenotyping of GPC3 CAR T cell products and post-infusion peripheral blood samples

GPC3-and 15.GPC3 CAR T cell products and peripheral blood samples were assessed with flow cytometry using BUV395-conjugated mouse anti-human CD4 (clone RPA-T4), BUV496-conjugated mouse anti-human CD8 (clone RPA-T8), BUV 737-conjugated mouse anti-human TIM-3 (clone 7D3), BV421-conjugated mouse anti-human CD25 (clone M-A251), BV480-conjugated mouse anti-human CD45RO (clone UCHL1), BV650-conjugated mouse anti-human CD279 (clone MIH4), BV711-conjugated mouse anti-human CD69 (clone FN50), BV786-conjugated mouse anti-human LAG3 (clone T47-530), BV605-conjugated mouse anti-human CD3 (clone SK7), APC-R700-conjugated mouse anti-human CD127 (clone HIL-7R-M21), FITC-conjugated mouse anti-human CD197 (CCR7) (clone 150503), PE-conjugated mouse anti-human CD271 (clone C40-1457), PerCP Cy5.5-conjugated mouse anti-human CD39 (clone TU66) and Viability Stain 780. PE-conjugated mouse IgG1 k was used as isotype control. All of the above antibodies are from BD Biosciences and had a dilution ratio of 1:20, except for anti-human CD271 (1:10), IgG1 k (1:10) and Viability Stain (1:1,000).

Transduction efficiency of peripheral blood samples was assessed in products and peripheral blood with the following antibodies. GPC3 CAR expression was measured with Alexa Fluor 647-Conjugated AffiniPure goat anti-mouse IgG, F (ab')$_2$ fragment specific (Polyclonal, Jackson Immunoresearch, 1:100 dilution), and IL-15 was measured with FITC-conjugated mouse anti-human NGFR (C40-1457, BD Biosciences, 1:20 dilution). Non-specific binding was mediated using monoclonal anti-bovine IgG antibody (catalogue no. BG18, Sigma-Aldrich, 1:200 dilution).

iNKTs and NK cells were assessed using BUV395-conjugated mouse anti-human CD4 (clone RPA-T4, 1:25 dilution), BUV496-conjugated mouse anti-human CD3 (clone UCHT1, 1:50 dilution), BUV805-conjugated mouse anti-human CD16 (clone 3G8, 1:50 dilution), BV421-conjugated mouse anti-human CD19 (clone SJ25C1, 1:50 dilution), BV480-conjugated mouse anti-human CD8 (clone RPA-T8, 1:50 dilution), BV750-conjugated mouse anti-human γδ TCR (clone 11F2, 1:50 dilution), FITC-conjugated mouse anti-human TCRα/β (clone WT 31, 1:10 dilution), PE-conjugated mouse anti-human iNKT (clone 6B11, 1:10 dilution), PerCP Cy5.5-conjugated mouse anti-human CD14 (clone MΦP9, 1:50 dilution), APC-R700-conjugated mouse anti-human CD56 (clone NCAM16.2, 1:20 dilution), Brilliant Stain Buffer Plus (1:20 dilution), Viability Stain 780 (1:1,000 dilution) and APC-conjugated mouse anti-human Vβ11 (clone C21, Cat. 1:12.5 dilution). All of the above antibodies are from BD Biosciences except for Vβ11, which is from Beckman Coulter Life Sciences.

Flow cytometry data were collected using Diva (v.9.1), and analysed with FlowJo (v.10.8.1) and GraphPad Prism (v.10.3). For pre-infusion CAR T cell products and post-infusion PBMCs, the lymphocyte region was selected on forward and side scatter, followed by hierarchical gating focused on populations of interest, as shown in Extended Data Fig. 10.

Cytotoxicity assessment

Target cells (2×10^6) were labelled with 0.1 mCi (3.7 MBq) ^{51}Cr and mixed with effector cells at the following effector:target ratios: 40:1, 20:1, 10:1, 5:1. Target cells were incubated in Click's medium with 5% glutamine and 1% fetal bovine serum. To determine maximum ^{51}Cr release, 5×10 ml^{-1} target cells were separately incubated in Triton X-100. Target and effector cells were incubated for 4 h, at which point supernatants were collected and radioactivity was measured in a gamma counter (PerkinElmer). The mean percentage of specific lysis of triplicate wells was calculated according to the following formula: (test release − spontaneous release)/(maximal release − spontaneous release) × 100.

Quantification of single-cell cytokine production

Cryopreserved CAR and 15.CAR T cell products were thawed in RPMI 1640 medium (Fisher, catalogue no. MT10040CV), supplemented with 10% fetal bovine serum (Sigma, catalogue no. F2442, 6 × 500 ml) and 1× Glutamax (Thermo, catalogue no. 35050061). Cells were then recovered overnight in complete RPMI medium with recombinant human IL-7 (10 ng ml^{-1}) and IL-15 (5 ng ml^{-1}, both from R&D Systems), at a density of 1×10^6 cells ml^{-1} in a 37 °C, 5% CO_2 incubator. Cells were stimulated with the HUH-7 tumour cell line at a 1:1 ratio of 1×10^6 cells ml^{-1} for 24 h at 37 °C and 5% CO_2. $CD4^+$/$CD8^+$ T cell subsets were then separated using anti-CD4 or -CD8 microbeads (Miltenyi, catalogue no. 130-045-101/130-045-201). Stimulated cells were labelled with membrane stain (1:500 dilution, IsoPlexis), resuspended in complete RPMI medium at a density of 1×10^6 cells ml^{-1} and then loaded into a human adaptive IsoCode Chip (IsoPlexis). Cells on the chip were incubated at 37 °C, 5% CO_2 for an additional 13.5 h on an IsoLight automation system (IsoPlexis). The polyfunctionality of T cells, defined as those cosecreting two or more cytokines, was analysed with IsoSpeak software across seven functional groups: T_H1 pro-inflammatory (GM-CSF, IFNγ, IL-2, IL-12, TNF); T_H2 pro-inflammatory (IL-4, IL-5, IL-7, IL-9, IL-13); chemoattractive (CCL11, IL-8, IP10, MCP1, MCP4, MIP1α, MIP1β, RANTES); regulatory (IL-10, IL-15, IL-22, TGFβ1); T_H17 pro-inflammatory (IL-1β, IL-6, IL-17A, IL-17F, IL-21); cytolytic (granzyme B, perforin); and other (sCD40L, sCD137). The PSI of T cells was computed using a prespecified formula, defined as the percentage of polyfunctional cells multiplied by the sum of mean fluorescence intensity of the proteins secreted by those cells. Functional groups of T cells were deconvoluted and visualized by three-dimensional *t*-distributed stochastic neighbour embedding and heatmap visualization.

Quantification of CAR T cells with quantitative PCR

Evaluation of CAR and iC9.NGFR-IL-15-expressing T cell persistence was assessed by calculating the copy number of either the GPC3 CAR or iC9.NGFR.IL-15 transgene, following extraction of genomic DNA from PBMCs with the QIAamp DNA Blood Minikit (QIAGEN) according to the manufacturer's manual, and measurement of transgene copy number by quantitative PCR with reverse transcription using the primer (forward, 5′-AGCTGCCGATTTCCAGAAGA-3′ and reverse, 3′-GCGCTCCTGCTGAACTTCA-5′) and probe (5′-AAGGA GGATGTGAACTGAGA-3′) sequences for the GPC3 CAR transgene and using the primer (forward, 5′-CTGGAATCTGGCGGTGGAT-3′ and reverse, 5′-CAAACTCTCAAGAGCACCGACAT-3′) and probe (5′-CGGAGTC GACGGATT-3′) sequences for the iC9.NGFR.IL-15 transgenes (Applied Biosystems) in a ABI Prism 7700 Sequence Detector (PerkinElmer). Copy number was normalized to 1 μg of PBMC DNA in patient samples, and transgene copy number was normalized per millilitre of patient peripheral blood at all time points.

Quantification of serum cytokine levels

Serum cytokine levels were measured with the Milliplex MAP magnetic bead-based multianalyte panel (EMD Millipore) on the Luminex 200

system (Luminex) with xPONENT (Luminex) software, according to the manufacturer's manual.

Rimiducid supply and dosing

Rimiducid, a chemical inducer of dimerization and activator of the iC9 safety switch, was manufactured and provided by Bellicum Pharmaceuticals. Rimiducid was diluted in normal saline in a volume appropriate for weight, and administered by intravenous infusion at the target dose by weight-adjusted doses of 0.004–0.030 mg kg^{-1}. Patients received only a single dose in this study.

scRNA-seq and processing

Cells were dissociated, and cell libraries prepared with the Chromium Next GEM Single Cell 5′ Reagent Kit v.2 kit (10X Genomics). Samples had viability of over 95%. Cells were labelled using a 10X Genomics Chromium Controller, and full-length complementary DNA was synthesized, barcoded and amplified by PCR. The KAPA Library Quantification kit (Roche) was used to quantify libraries, which were sequenced using NovaSeq 6000 (Illumina) at a sequencing depth of around 500 million reads. The GPC3 CAR sequence has a murine-derived, GPC3-specific, single-chain variable fragment and a MMLV packaging signal. This sequence was indexed, together with the human reference genome (v.GRCh38.p13), to generate a chimeric reference before data preprocessing and read alignment. Alignment to the chimeric reference followed the 10X Genomics standard, using Cell Ranger (v.7.1.0) and tertiary analysis with Seurat tools. Cells with raw UMI above zero matching the GPC3 CAR sequence were identified as CAR^+ cells. Before cell clustering, quality control was conducted in Seurat[39] (v.4.0). Genes detected in fewer than ten cells, cells with fewer than 200 profiled genes and more than 10% of mitochondrial raw UMIs were removed to exclude low-quality or dying cells. Cells with more than 7,000 genes were also excluded. Doublets were identified using DoubletFinder v.2.0. Because of the sparsity of CAR T cells—particularly in the CAR cohort—spike-in-primers were used in postlibrary preparation to increase the detection limit of CAR T cells in scRNA-seq assays with limited CAR T representation. The following sequences were used to amplify the GPC3 CAR transgene: 5′-GATCTACACTCTTTCCCTACACGACGC, 3′-TAAACTTCTGGGAATATGCTGTATCCCCGGTTT. Following clean-up, enzymatic fragmentation and size selection were used to generate variable-length fragments that collectively span the entire transcript. Library construction was carried out by end repair, A-tailing, adaptor ligation and PCR amplification. UMI counts were log normalized with a scale factor of 10,000. The 2,000 most variable marker genes were retained and scaled (linear transformation) for clustering and integration. CAR^+ cells in pre-infusion product samples were integrated using the algorithm harmony v.1.2 (ref. 46). When clustering CAR T product samples, we performed principal component analysis on the scaled data and unsupervised Louvain clustering analysis with a resolution of 0.5. A total of 12 clusters were identified from 24 pre-infusion product samples. Cells in each cluster were projected onto a two-dimensional UMAP. When available, CAR^+ cells from pre-infusion product-, peripheral blood- and tumour biopsy-derived data were integrated using the algorithm harmony. B cells, red blood cells and monocytes were filtered out by removal when HBB, CD79A, MS4A1, CD19, CD22, CD14 and MS4A7 reads were above 0. Clonality assessment was performed by 10X Genomics V(D)J, and TCR-enriched libraries sequenced with NovaSeq 6000 (Illumina). Reads were processed using the Cell Ranger v.7.1.0 function cellranger multi. Cell clonality among samples and alluvial plots was generated using the scRepertoire v.2.0.3 function clonalCompare(cloneCall = "aa", graph = "alluvial")[47]. For clonal analyses, clonal expansion was defined as variable-diversity joining sequences shared by at least one cell within the tumour biopsy.

Differential gene and gene set expression analysis

Differential gene expression in product versus peripheral blood in the IL-15.CAR versus CAR evolution comparison was performed as follows. We randomly downsampled each donor down to 125 single cells. Raw read counts from each donor were then summed from all cells by gene using the Seurat function PseudobulkExpression(pb.method = "aggregate"). Differential gene expression between product and peripheral blood samples was calculated using DESeq2 (ref. 48) for IL-15.CAR and CAR separately. The DESeq2 parameters used for these analyses were DESeq(test = "LRT", sfType = "poscounts", useT = T, reduced = ~1). Shrinkage of effect size was calculated using the DESeq2 function lfcShrink(type=apeglm, svalue = T). We performed this resampling procedure 200 times, then values were averaged to produce *P* value estimates. Fold change estimates were produced by comparison of psuedobulk profiles across CAR T cells in each sample, using a psuedocount of 1. For cluster proportion statistical analysis, two-tailed *P* values were calculated using a hypergeometric distribution, comparing the composition of each cluster (responder versus non-responder cells) with that of the total cell population. Differential gene expression in product versus biopsy in the responder versus non-responder evolution comparison was performed as described above, with the following differences: cells from each donor were randomly downsampled to match the size of the cohort with fewest identified CAR T cells. Gene Ontology gene sets with false discovery rate below 0.05 for up or down enrichment were identified using gene set enrichment analysis. Differential gene expression in tumour responders versus non-responders was performed using the Seurat function FindMarkers (test.use = "wilcox_limma", min.pct = 0.3, min.diff.pct = 0.1). Average expression of gene sets[49] at the single-cell level was calculated using the Seurat function AddModuleScore().

Statistical analysis

All patients were included in both primary and safety analyses. Descriptive statistics were used to describe phenotypic data and T cell expansion. Plots of growth curves demonstrating measurements over time among patients were generated to visualize patterns of immune reconstitution. Comparisons were made between groups using the Wilcoxon rank-sum test or *t*-test, whichever was appropriate, for continuous variables, and the Fisher exact test for categorical variables. Changes from baseline to follow-up measures were compared using the Wilcoxon signed-rank test. Confidence intervals for relative risk were calculated with Koopman asymptomatic score, and *P* values estimated by Fisher's exact test. Statistics were computed using GraphPad Prism 10.3 (GraphPad Software). Differences were considered significant at $P < 0.05$.

Reporting summary

Further information on research design is available in the Nature Portfolio Reporting Summary linked to this article.

Data availability

All requests for additional raw and analysed data should be directed to A.H. Patient-related data not included in the paper were generated as part of the clinical trial and may be subject to patient confidentiality. Following removal of all human research participant identifiers, raw data for single-cell sequencing were deposited in the Gene Expression Omnibus under accession no. GSE253352.

45. Li, W. et al. Redirecting T cells to glypican-3 with 4-1BB zeta chimeric antigen receptors results in Th1 polarization and potent antitumor activity. *Hum. Gene Ther.* **28**, 437–448 (2017).
46. Korsunsky, I. et al. Fast, sensitive and accurate integration of single-cell data with Harmony. *Nat. Methods* **16**, 1289–1296 (2019).
47. Borcherding, N., Bormann, N. L. & Kraus, G. scRepertoire: an R-based toolkit for single-cell immune receptor analysis. *F1000Res.* **9**, 47 (2020).
48. Love, M. I., Huber, W. & Anders, S. Moderated estimation of fold change and dispersion for RNA-seq data with DESeq2. *Genome Biol.* **15**, 550 (2014).
49. Liberzon, A. et al. The Molecular Signatures Database (MSigDB) hallmark gene set collection. *Cell Syst.* **1**, 417–425 (2015).

Acknowledgements We thank E. Di Pierro for helpful editing of the manuscript. We also thank C. Zhang for preliminary assessment of the scRNA-seq datasets. Funding was provided by the following: R01CA258866 (A.H.), R35CA220500 (J.M.M.), R01GM143243 (N.V.), T32GM136554 (A.B.A.) and R21CA286257 (P.S.) were from NIH; RP190160 (A.H.), RP180785 (A.H.), RP200584 (P.L.), RP230120 (P.S.) and RP180674 (D.L.-T.) were from the Cancer Prevention and Research Institute of Texas; funding was also provided by the V Foundation (A.H.); Cookies for Kids' Cancer Foundation (A.H.); the National Gene Vector Biorepository at Indiana University from the National Heart Lung and Blood Institute and National Cancer Institute contract (nos. HSN261201500003I, 75N92019D00018 and HSN261201500003I); and Task Order (nos. HHSN26100077 and HHSN26100077).

Author contributions Conceptualization was the responsibility of A.H., M.K.B., N.V. and P.S. Data curation was undertaken by A.B.A., A.H., A.M. and P.S. A.B.A., A.H., A.M., J.P., D.M., J.M.M., K.P., D.S., M.K.B. and P.S. carried out formal analysis. A.H. acquired funding. Investigation was performed by A.H., D.S., P.L., T.A. and C.A.R. Regulatory approval and vector availability were undertaken by A.H., G.D., S.G., M.K.B., H.E.H. and B.J.G. A.B.A., A.H., J.F., A.M., D.S. and P.S. carried out the methodology. A.H., L.S.M. and P.S. were responsible for resources. Software was overseen by A.B.A., A.H., A.M. and P.S. A.H., P.S., B.J.G., H.E.H. and M.K.B. supervised. A.B.A., A.H. and A.M. performed visualization. A.H. wrote the original draft. All authors contributed to writing review and editing.

Competing interests A.H., G.D., S.G. and L.S.M. have patents related to GPC3 CARs. A.H. is consultant for Waypoint Bio and serves on the Scientific Advisory Board of CARGO Therapeutics. A.H. has equity in CARGO. A.H. and L.S.M. received research support from Kuur/Athenex Therapeutics. A.H. and P.R. have a pending patent application related to cytokine co-expression in CAR T cells. N.V. is cofounder of CellChorus and AuraVax Therapeutics. M.K.B. has equity in AlloVir Inc., Marker Therapeutics, Tessa Therapeutics Ltd and March Biosciences, and serves on advisory boards for Marker Therapeutics, Allogene, Walking Fish, Abintus, Tessa Therapeutics, Athenex, Onk Therapeutics, Coya Therapeutics, Triumvira, Adaptimmune, Vor Therapeutics, Tscan, Kuur, Memgen and Turnstone Biologics Ltd. M.K.B. is the inventor of the iC9 safety switch. M.K.B. received royalties from Bellicum Pharmaceuticals. H.E.H. has equity in AlloVir Inc. and Marker Therapeutics and share options in CoRegen; has served on advisory boards for March Biosciences, Fresh Wind Biotechnologies, Kiadis, GSK, Marker Therapeutics and Tessa Therapeutics; and has received research support from Tessa Therapeutics and Kuur Therapeutics. S.G. is coinventor on patent applications in the fields of cell or gene therapy for cancer, and is a member of the Scientific Advisory Board of Be Biopharma and CARGO, and of the Data and Safety Monitoring Board of Immatics. B.J.G. owns QB Regulatory Consulting which has, or has had, agreements with Tessa Therapeutics, AlloVir (including equity), Marker Therapeutics, Lokon Pharma and March Biosciences. C.A.R. has participated in advisory boards for Novartis, Genentech and CRISPR Therapeutics, and has received research funding from Athenex and Tessa Therapeutics. P.L. served on the advisory board for Janssen Therapeutics and receives research funding from Marker Therapeutics. A.M. has equity in Immunai Inc. The other authors declare no competing interests. N.L. received research support from Tessa Therapeutics.

Additional information

Supplementary information The online version contains supplementary material available at https://doi.org/10.1038/s41586-024-08261-8.

Correspondence and requests for materials should be addressed to Andras Heczey.

Peer review information *Nature* thanks Phillip Darcy, Frederick Locke and Donald O'Rourke for their contribution to the peer review of this work. Peer reviewer reports are available.

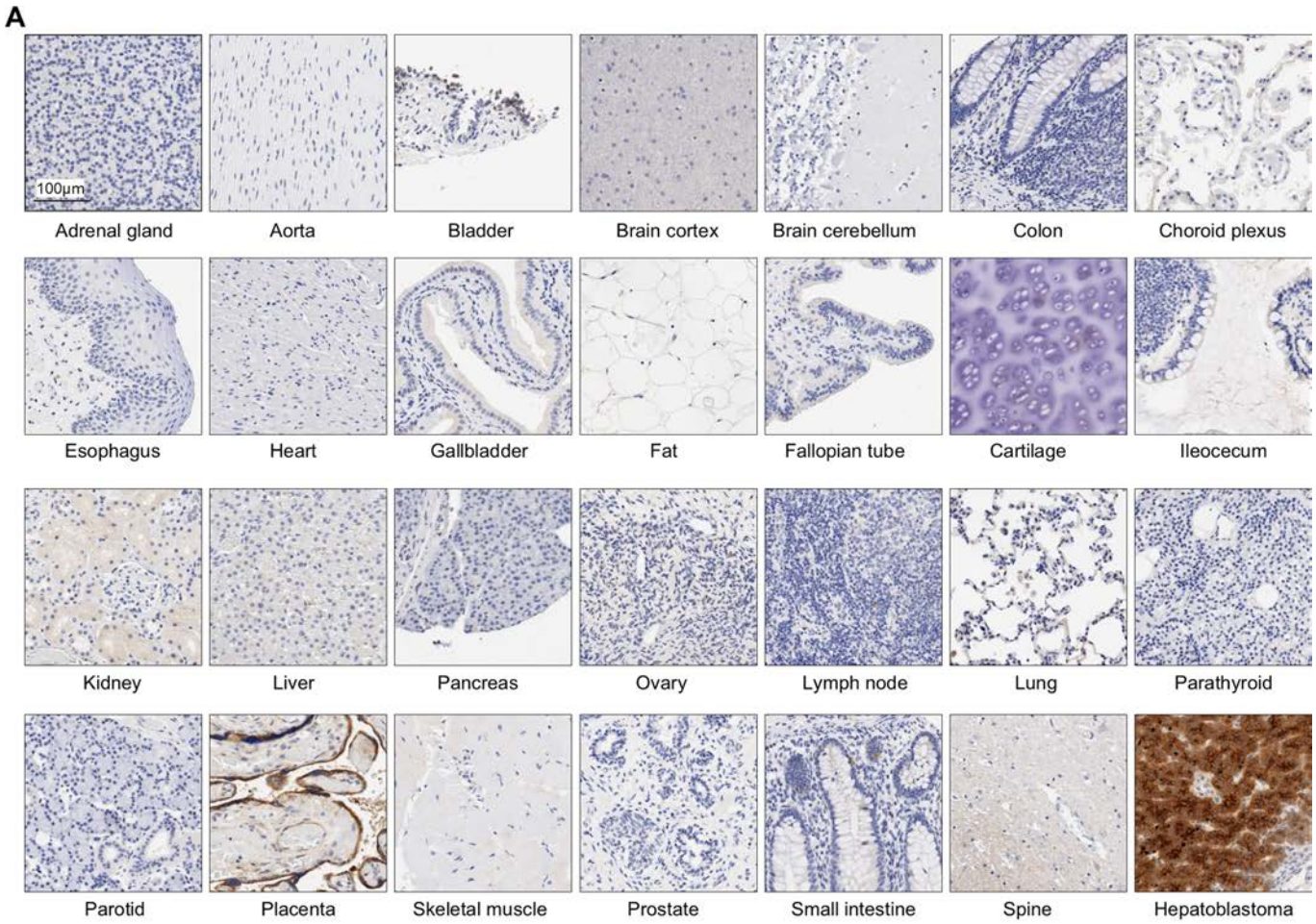

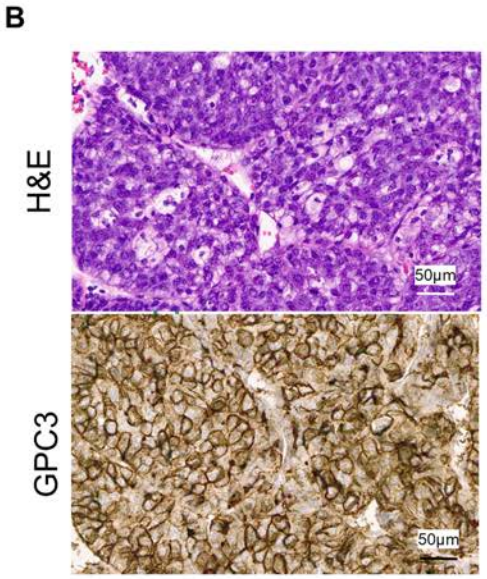

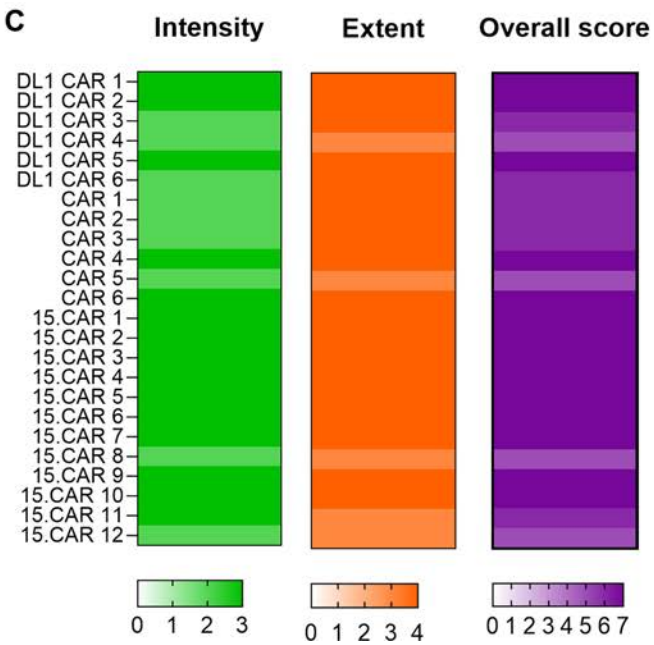

Extended Data Fig. 1 | Assessment of GPC3 expression: GPC3 expression was measured by Immune-histochemistry. A. Expression of GPC3 in pediatric tissue array – samples from hepatoblastoma and placenta were used as positive controls. Scale bar = 100 µm *(19)*. **B.** Example of an enrollment sample from Patient 15.CAR 2. For A and B, Staining performed once in the clinical pathology laboratory with appropriate positive and negative controls. **C.** Intensity, extent and cumulative GPC3 expression scores for enrolled patients as previously described *(20)*.

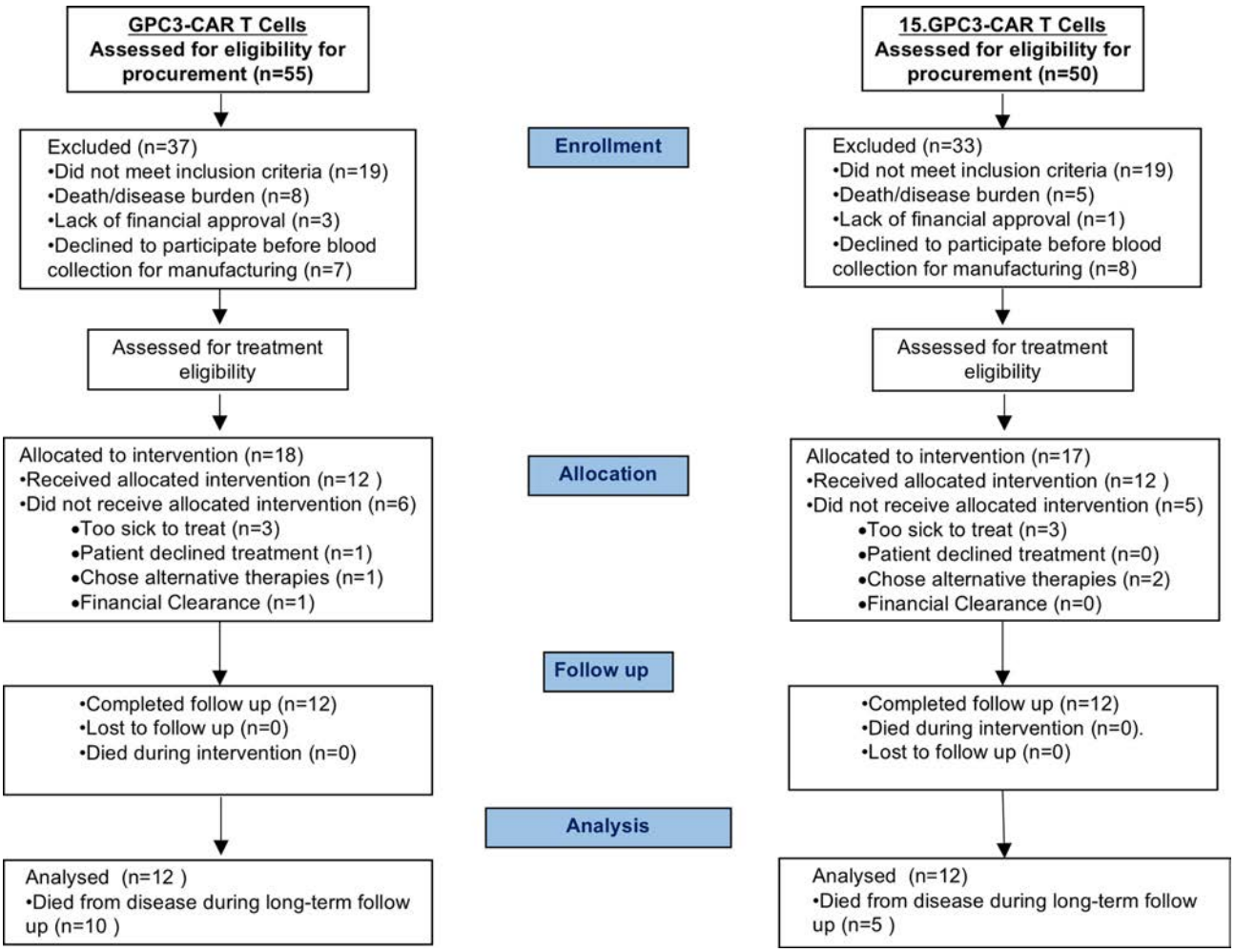

Extended Data Fig. 2 | Patient accrual and enrollment. Consort diagram summarizing patients referred, enrolled, and treated on GPC3- and 15.GPC3-CAR T cell studies.

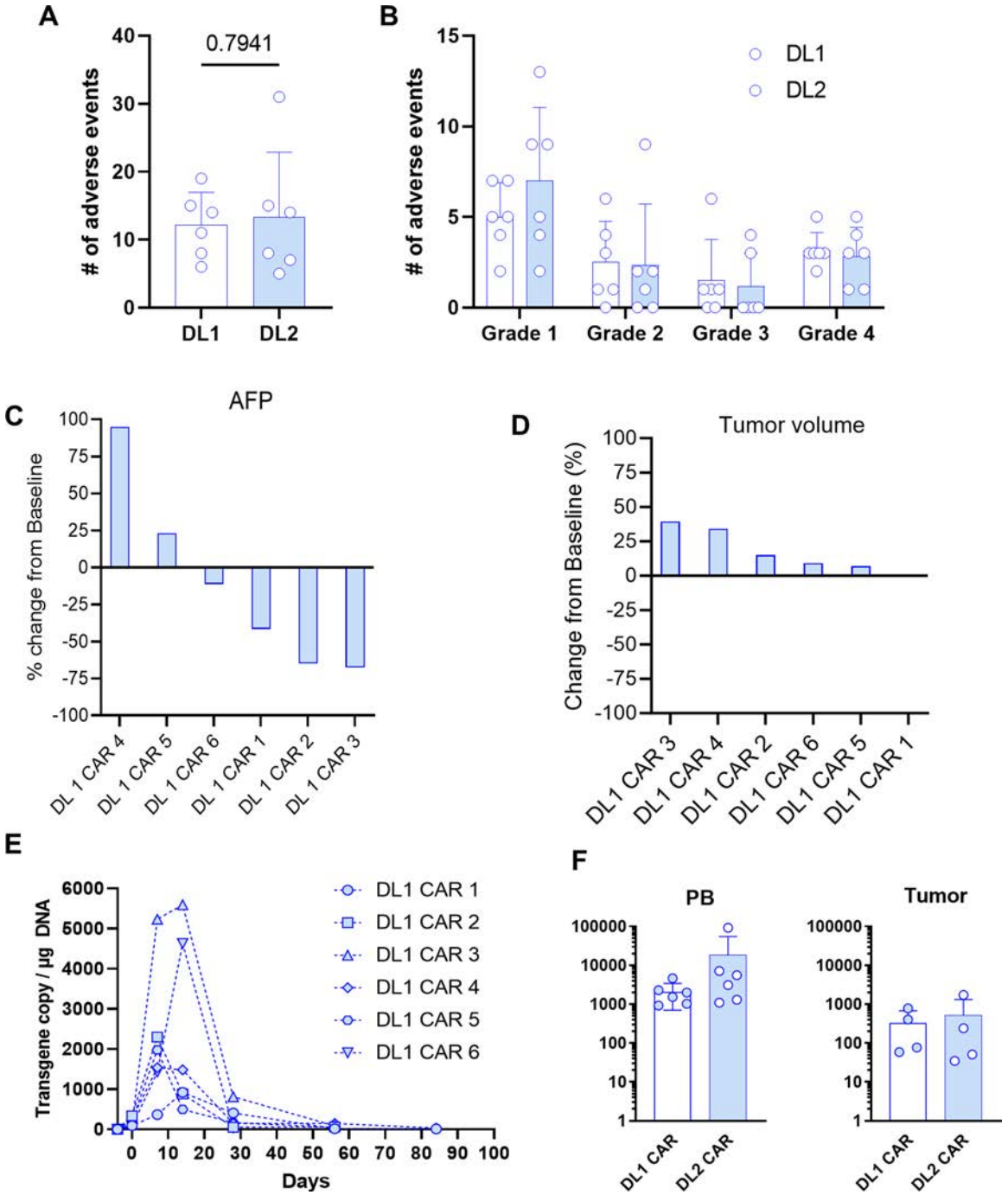

Extended Data Fig. 3 | Safety, antitumor activity and peripheral blood and tumor kinetics of patients treated with CAR T cells DL1 and DL2. A. Total number adverse events and **B**. Number of adverse events for each patients treated at $1 \times 10^7/m^2$ (DL1, n = 6) and $3 \times 10^7/m^2$ (DL2, n = 6). **C**. Change in serum AFP levels in patients treated at DL1 dose of GPC3-CAR T cells. **D**. Change in tumor volume of these patients. **E**. Peripheral blood transgene copy numbers at indicated timepoints for patients treated at DL1 with GPC3-CAR T cells. **F**. Comparison of transgene copy numbers in PB (left) and tumor (right) of GPC3-CAR T cell levels treated on DL1 (n = 4) and DL2 (n = 4). Comparisons by two-tailed, unpaired T test and two-way ANOVA with Šidák correction. Data represented as mean ± SD.

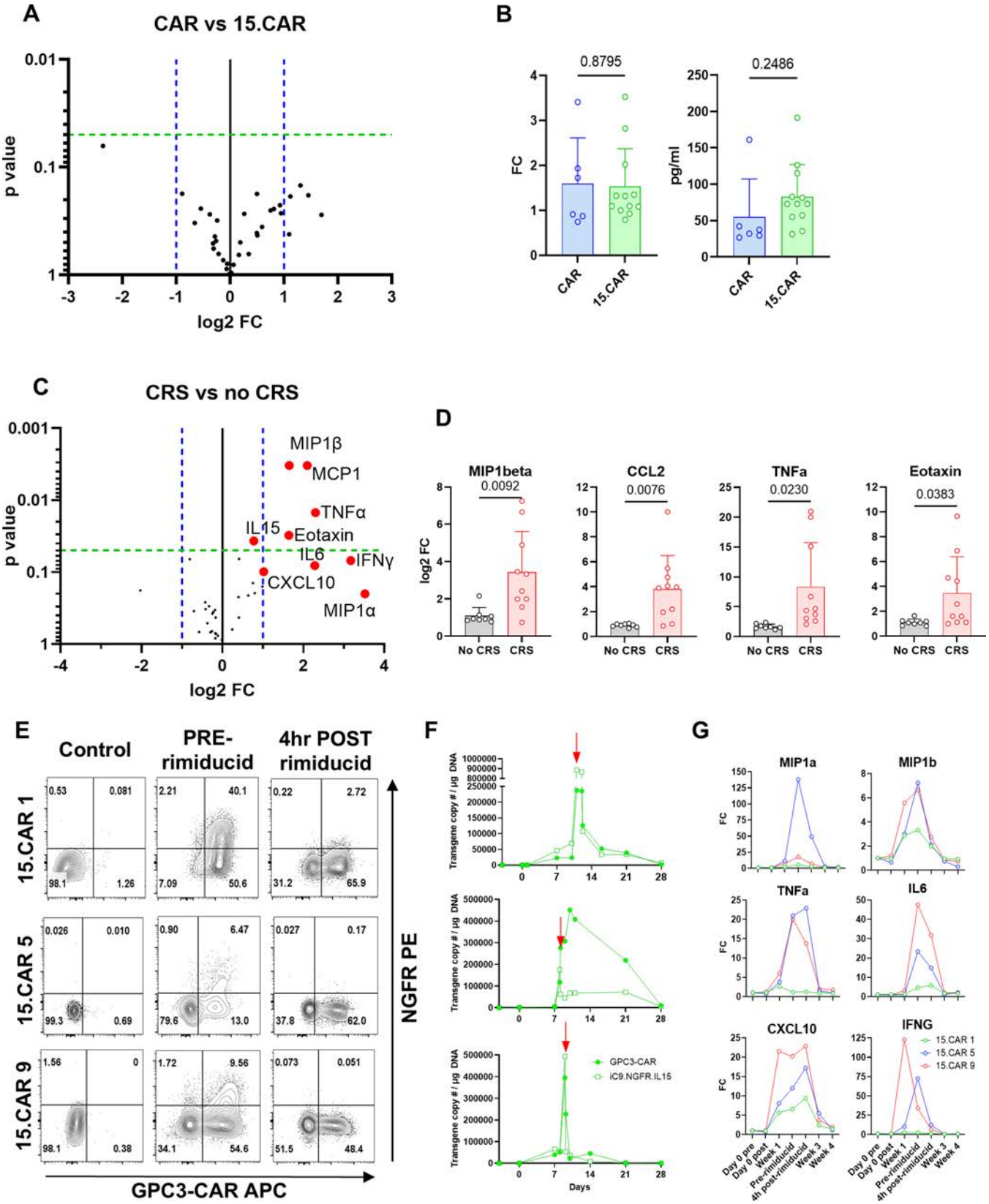

Extended Data Fig. 4 | See next page for caption.

Extended Data Fig. 4 | Serum cytokine and chemokine kinetics post-infusion. Levels of chemokines and cytokines were quantified on Day -4, Day 0 and weekly until Day 28. Fold change (FC) was calculated from Day 0 (baseline) to assess changes dependent on CAR T and 15.CAR T cell infusions. **A**. Comparison of FC from baseline to peak concentration for all measured analytes. **B**. Fold change and peak expansion concentration of IL15 in CAR (n = 6) vs 15.CAR (n = 12) treated patients. **C-D**. Differentially expressed cytokines in patients with (n = 10) and without CRS (n = 8). Overview of all measured analytes (C) and individual cytokines with at least two-fold, statistically significant increase (D). Two-tailed, unpaired T test. Data represented as mean ± SD. **E-G**. Proportions of GPC3-CAR and iC9.NGFR.IL15 expressing T cells quantified by flow cytometry (**E**) and qPCR (**F**, red arrows indicate timing of rimiducid administration) and changes in concentrations of indicated serum cytokines (**G**) in peripheral blood of patients treated with rimiducid, the chemical inducer of the iC9 safety switch.

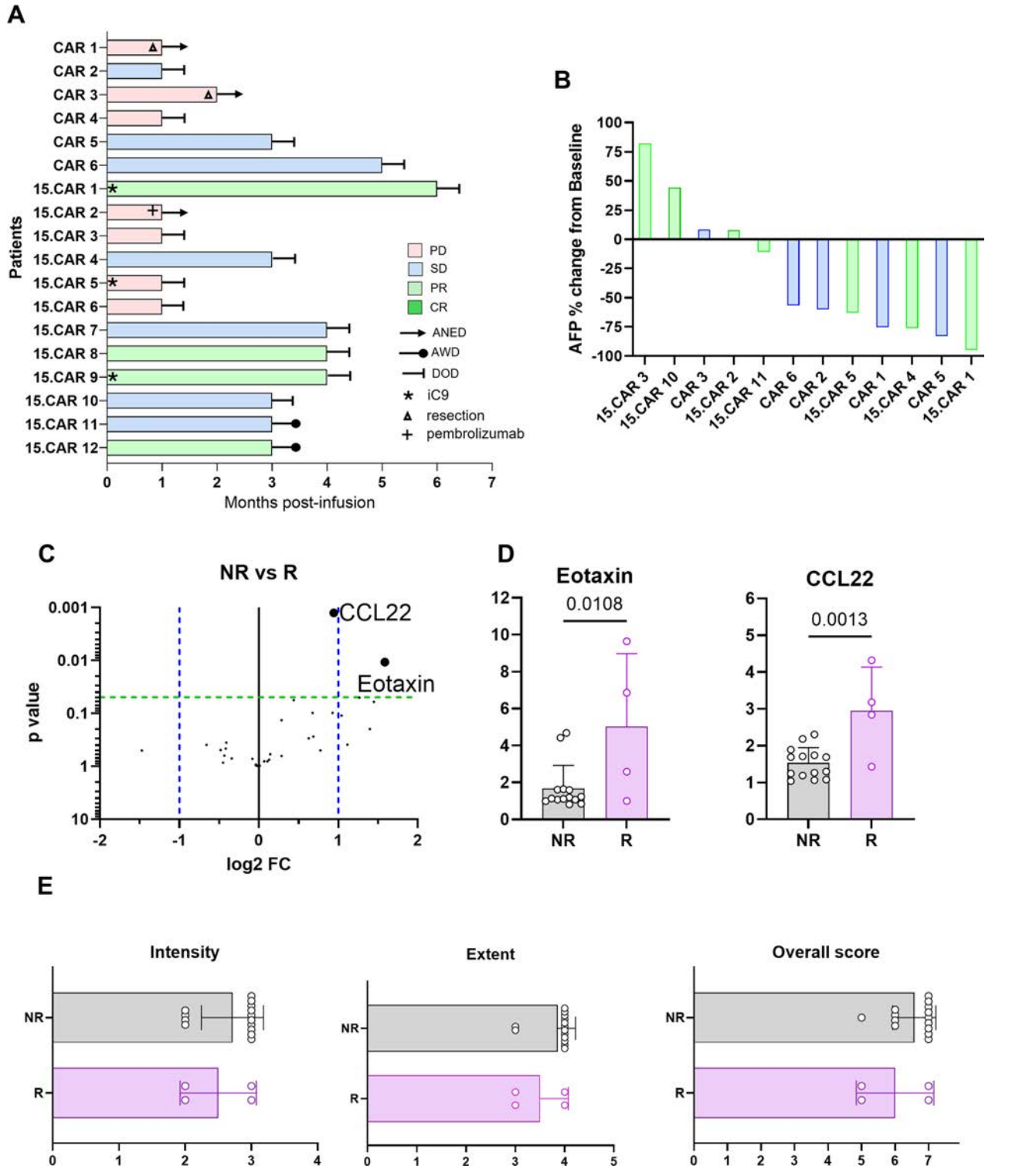

Extended Data Fig. 5 | Antitumor response characteristics in patients treated with CAR and 15.CAR T cells. A. Long term outcome of treated patients with additional treatments shown for those with Alive with no evidence of disease (ANED). Patients needing the iC9 safety switch indicated. AWD: alive with disease. DOD: Died of disease. **B**. Serum alpha-feto protein (AFP) was measured in the CLIA certified clinical laboratory before and after CAR T cell infusions. Waterfall plot representing changes in AFP concentration from baseline in patients with AFP secreting tumors. **C**. Differentially expressed cytokines in non-responders (NR) vs responders (R) according to RECIST criteria. **D**. Comparison of individual cytokines with at least two-fold, statistically significant increase in responder (R, n = 4) and non-responder (NR, n = 14) patients. **E**. Comparison of GPC3 expression of tumors from responder (R, n = 4) and non-responder (NR, n = 14) patients. Two tailed, unpaired T test. Data represented as mean ± SD.

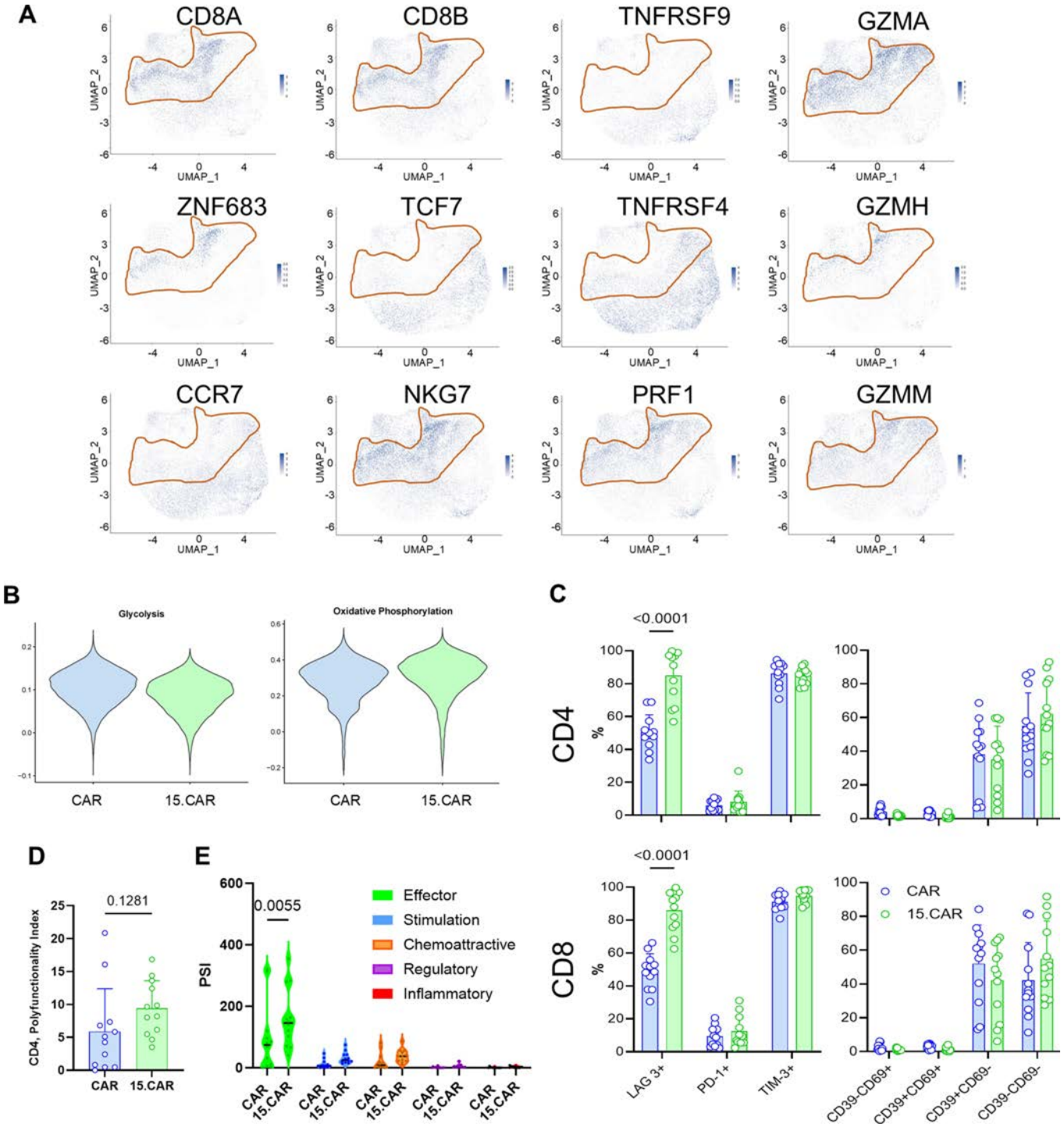

Extended Data Fig. 6 | Gene expression, cell surface marker phenotype and polyfunctionality of CAR vs 15.CAR T cell infusion products. A. UMAP projections showing indicated genes for individual cells after combining data from all CAR and 15.CAR T cell infusion products. Region outlined with orange corresponds to 15.CAR enriched cells. Cells were stained for expression of indicated cell surface markers. **B**. Metabolic profile of CAR and 15.CAR products using scRNAseq. **C**. CD4 (top) and CD8 (bottom) positive CAR T cells' expression of exhaustion (LAG3, PD1, TIM3) markers and proportion of CD39/CD69 subsets in all CAR (n = 12) and 15.CAR (n = 12) T cell infusion products. Comparison by two-way ANOVA with Šidák correction for multiple comparisons. **D-E**. Manufactured CAR (n = 12) and 15.CAR (n = 12) cells were evaluated by the Isoplexis, single cell cytokine detection system. (D). Polyfunctionality index of CD4 subset and (E). Polyfunctionality strength index of the indicated products. Two-way ANOVA with Šídák correction. Data represented as mean ± SD.

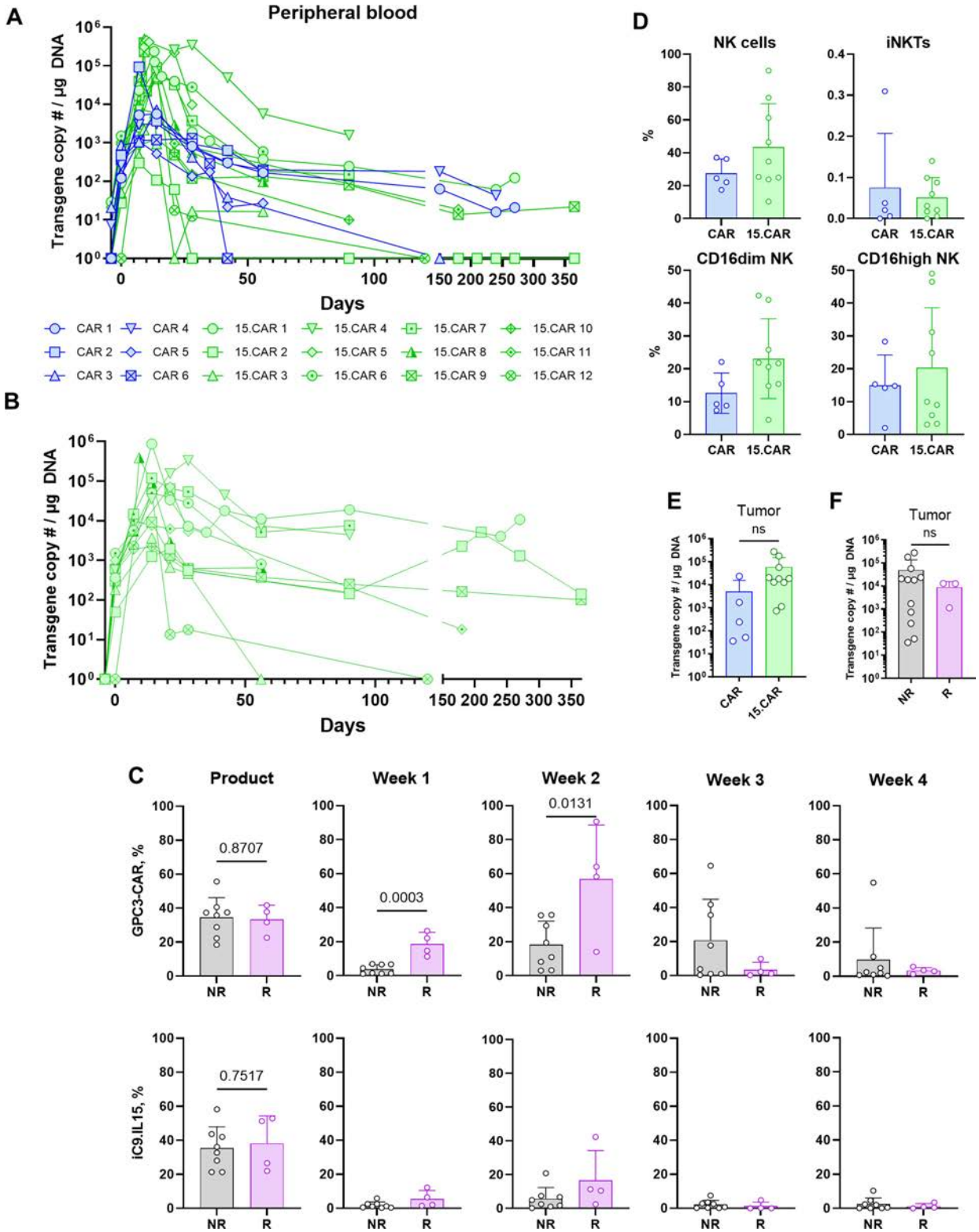

Extended Data Fig. 7 | Expansion, persistence and trafficking of CAR vs 15.CAR T cells post-infusion. Expansion and persistence of infused cell populations were quantified with qPCR. **A-B**. Transgene copy numbers for the GPC3-CAR (A) and iC9.NGFR.IL15 (B). **C**. Comparison of CAR and iC9.NGFR.IL15 transgene expression in non-responder (NR, n = 8) vs responder (R, n = 4) products and peripheral blood samples at indicated timepoints by flow cytometry. **D**. CAR- negative NK and iNKT subsets in peripheral blood isolated from patients infused with CAR (n = 5) or 15.CAR (n = 9) measured by flow cytometry. **E-F**. GPC3-CAR transgene frequencies in tumor biopsies in CAR (n = 5) vs 15.CAR (n = 10) groups (E) and in R (n = 3) vs NR (n = 12) groups (F). Two-tailed, unpaired T test. Data represented as mean ± SD.

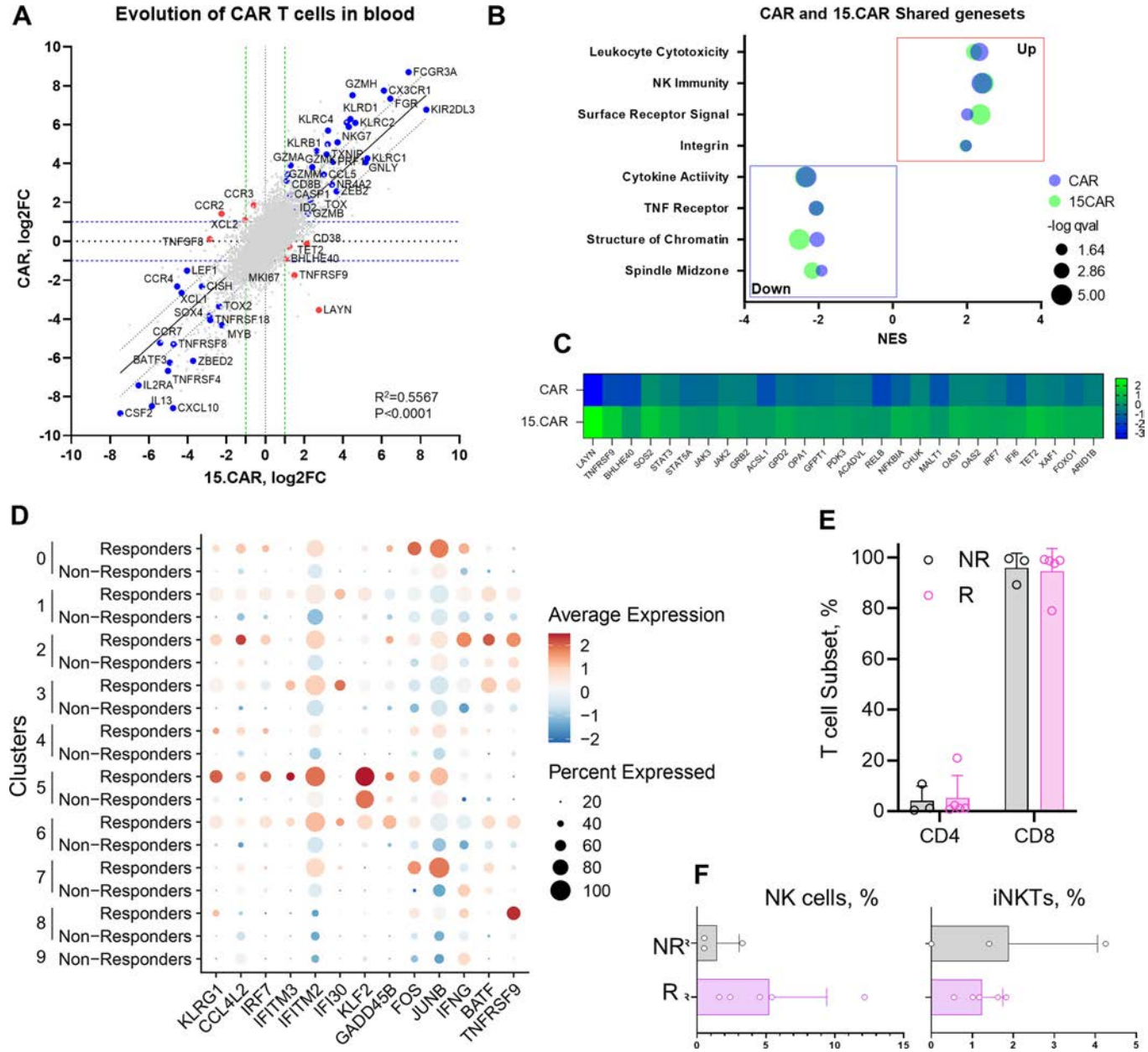

Extended Data Fig. 8 | Gene expression evolution in CAR and 15.CAR T cells post-infusion. The transcriptomic profile of Infusion products and peripheral blood CAR and 15.CAR T cells (A-C) or infusion products and tumor infiltrating 15.CAR T cells (D) were interrogated with single cell RNA sequencing. Differentially expressed genes (DEGs) for indicated groups were determined by comparing the product and post-infusion samples. **A**. DEGs from infusion product to peripheral blood represented by log2 fold change (log2FC) in CAR (y axis) vs 15.CAR (x axis) T cells. Linear regression. **B**. Selected gene sets enriched in CAR vs 15.CAR T cells in PB. **C**. Heatmap representing a subset of DEGs from the pre-infusion product to PB comparison in CAR vs. IL15.CAR. **D**. Selected cluster specific DEGs in 15.CAR T cells captured in tumors post-infusion. Cluster 9 contains only Non-responder cells. **E**. CD4/8 T cell subset composition of CAR+ TILs in responder (R, n = 5) and non-responder (NR, n = 3) tumor biopsies post-infusion in the 15.CAR group. **F**. CAR-negative lymphocyte subset composition in responder (R, n = 5) and non-responder (NR, n = 3) tumor biopsies post-infusion in the 15.CAR group. Data represented as mean ± SD.

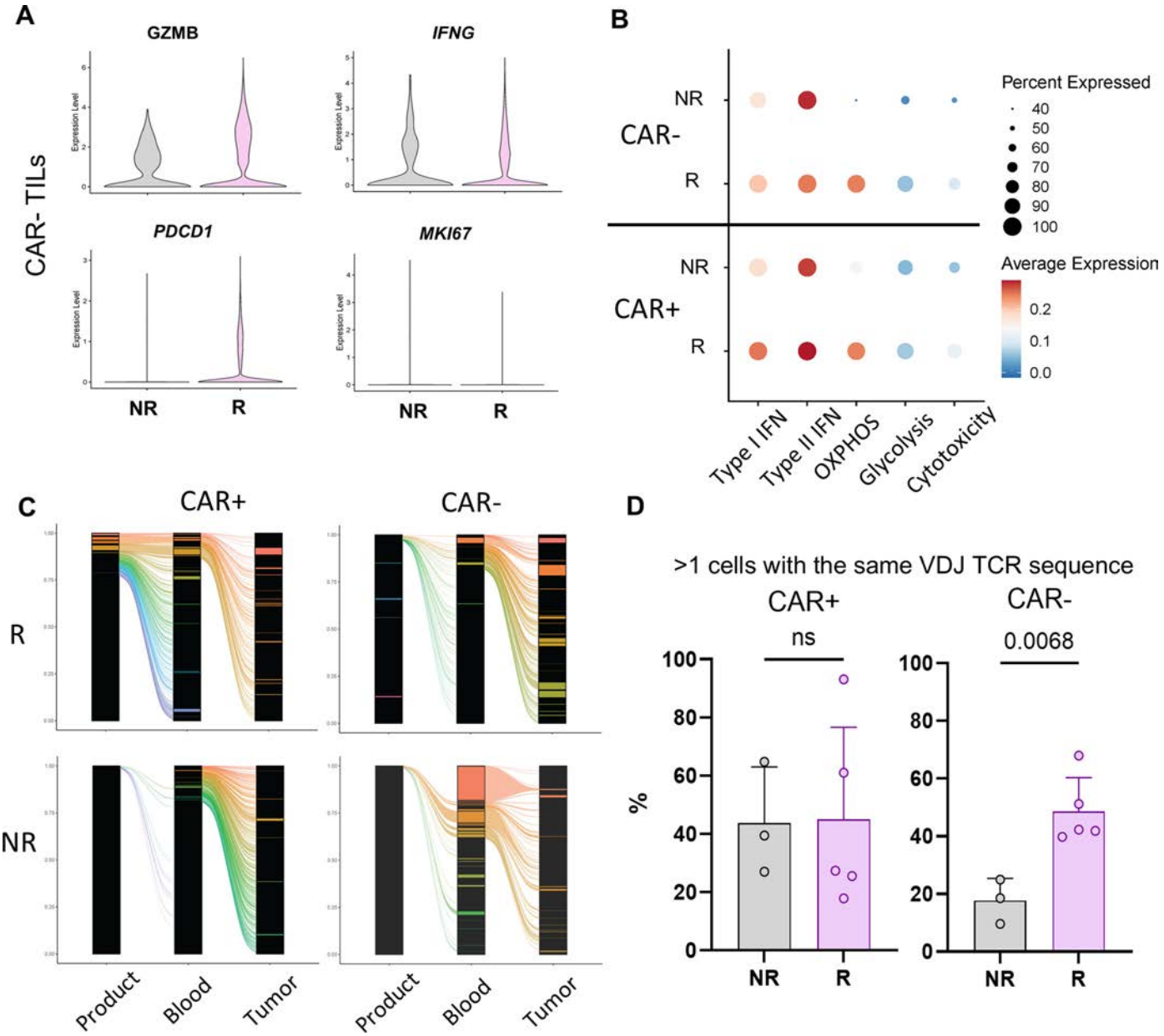

Extended Data Fig. 9 | Characteristics of CAR+ and CAR- T cells in patients post-infusion. A. Expression of indicated genes in CAR-negative, bystander tumor infiltrating lymphocytes (TILs). **B**. Gene expression signatures in CAR-positive and CAR-negative TILs in tumors of responder (R) and non-responder (NR) patients. **C**. T cell clones of CAR-positive and CAR-negative subsets from product, blood and tumor samples. Colored lines correspond to VDJ clones trackable between product / peripheral blood and tumor-derived T cells. **D**. Proportion >1 cells with the same VDJ TCR sequence of responder (R, n = 5) and non-responder (NR, n = 3) tumor infiltrating CAR-positive and CAR-negative T cell subsets. Two-tailed, unpaired T test, data represented as mean ± SD.

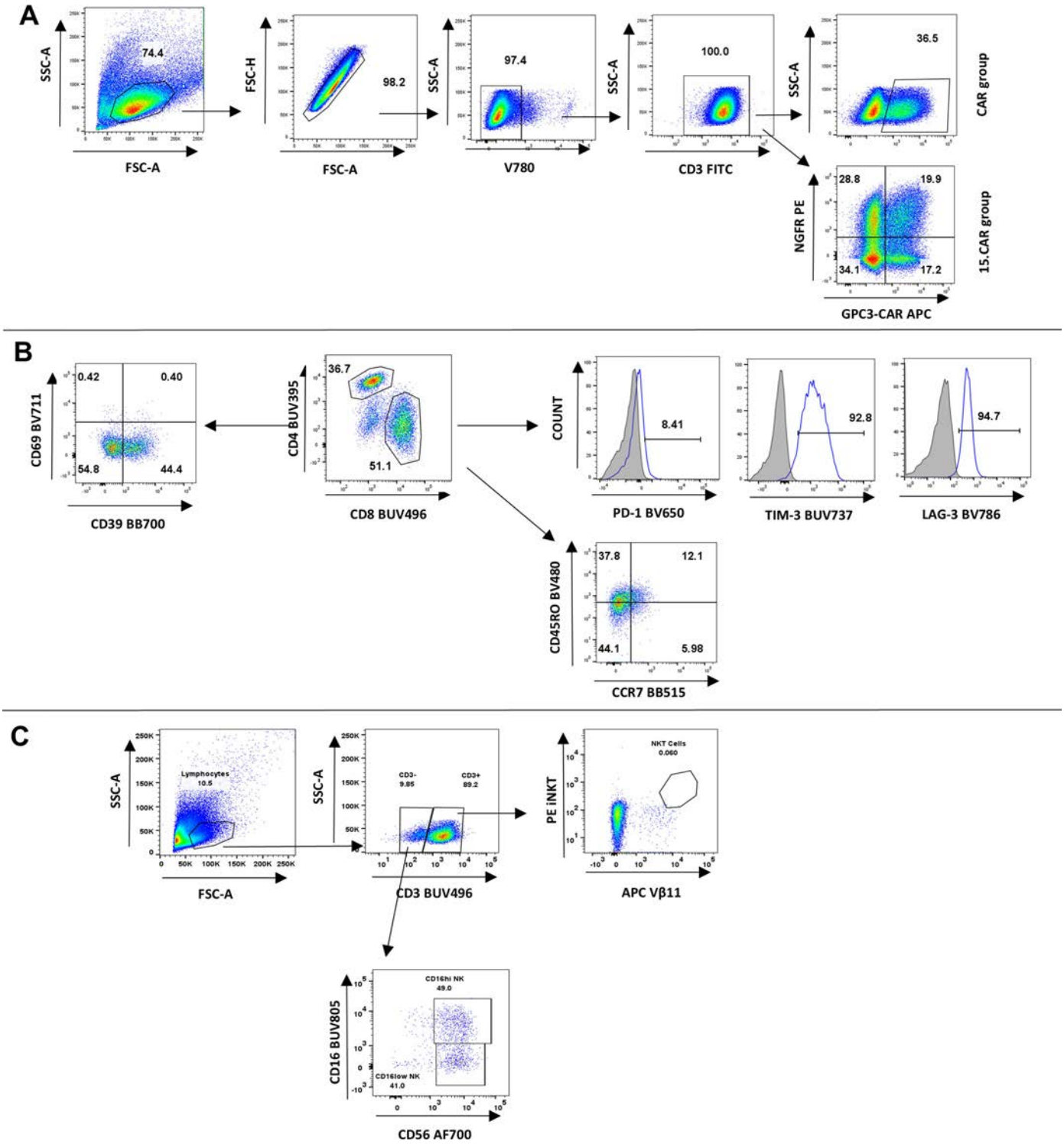

Extended Data Fig. 10 | Gating strategy for product and peripheral blood phenotyping. Patient-derived and product samples were processed and stained with indicated fluorochrome-conjugated antibodies. **A**. After gating on live cells and removing duplets, the T cell population was defined as CD3+ and evaluated for CAR and IL-15 expression based on Anti Fab APC and NGFR PE, respectively. **B**. Manufactured products were further characterized based on gating strategy in A. The CAR+ subset was further analyzed to determine CD4/CD8, memory, and exhaustion markers. **C**. Gating strategy to characterize NK and iNKT subsets in peripheral blood.

Extended Data Table 1 | Patient characteristics

DOSE LEVEL 1 - Patient characteristics						
Patient ID	**Age (years)**	**Gender**	**Tumor**	**Extrahepatic metastases**	**Site(s) of Active Disease**	**Response**
DL1.CAR 1	3	Female	HB	+	Liver and lungs	Progressive disease
DL1.CAR 2	7	Female	HC-NOS	+	Lungs	Stable disease
DL1.CAR 3	13	Female	HB	+	Lungs	Progressive disease
DL1.CAR 4	68	Female	HCC	+	Liver, retroperitoneal nodes, and para-aortic mass	Progressive disease
DL1.CAR 5	67	Female	HCC	+	Liver and bone	Stable disease
DL1.CAR 6	50	Female	HCC	+	Liver and lungs	Stable disease
DOSE LEVEL 2 - Patient characteristics						
CAR 1	4	Male	HB	+	Lungs	Progressive disease
CAR 2	4	Male	HB	+	Lungs	Progressive disease
CAR 3	4	Male	HB	+	Lungs	Stable disease
CAR 4	62	Female	HCC	+	Liver and lungs	Progressive disease
CAR 5	63	Male	HCC	+	Liver with invasion of portal node and abdominal wall	Stable disease
CAR 6	72	Male	HCC	+	Liver and retroperitoneal lymph node	Stable disease
15.CAR 1	20	Male	HCC	+	Liver, lungs, and bone	Partial response
15.CAR 2	8	Female	HCC	+	Liver and lungs	Progressive disease
15.CAR 3	10	Male	HCC	+	Liver and lungs	Progressive disease
15.CAR 4	11	Female	HC-NOS	+	Liver and lungs	Stable disease
15.CAR 5	11	Male	HC-NOS	-	Liver	Progressive disease
15.CAR 6	6	Female	WT	+	Liver and Lungs	Progressive disease
15.CAR 7	20	Female	NET	+	Pancreas, Liver	Stable disease
15.CAR 8	11	Male	ERMS	+	Right Nasopharynx	Partial response
15.CAR 9	68	Male	HCC	-	Liver	Partial response
15.CAR 10	65	Male	HCC	+	Liver and Retroperitoneal lymph node	Stable disease
15.CAR 11	32	Male	YST	+	Mediastinum, Axillary nodes, and Bone	Stable disease
15.CAR 12	69	Male	HCC	-	Liver	Partial response

Patients infused CAR on DL1 (top section) and with CAR or 15.CAR T cell on DL2 (bottom section) are described for general demographics, underlying malignancy, extent of disease and response to therapy.
HCC: Hepatocellular carcinoma. HC-NOS: Hepatocellular neoplasm not otherwise specified. Cy: cyclophosphamide. Flu: Fludarabine. YST: Yolk sac tumor; WT: Wilms Tumor; NET: neuroendocrine tumor of the pancreas, ERMS: Embryonal rhabdomyosarcoma.

nature portfolio

Corresponding author(s): Andras Heczey, MD

Last updated by author(s): Aug 22, 2024

Reporting Summary

Nature Portfolio wishes to improve the reproducibility of the work that we publish. This form provides structure for consistency and transparency in reporting. For further information on Nature Portfolio policies, see our Editorial Policies and the Editorial Policy Checklist.

Statistics

For all statistical analyses, confirm that the following items are present in the figure legend, table legend, main text, or Methods section.

n/a	Confirmed
☐	☒ The exact sample size (*n*) for each experimental group/condition, given as a discrete number and unit of measurement
☐	☒ A statement on whether measurements were taken from distinct samples or whether the same sample was measured repeatedly
☐	☒ The statistical test(s) used AND whether they are one- or two-sided *Only common tests should be described solely by name; describe more complex techniques in the Methods section.*
☐	☒ A description of all covariates tested
☐	☒ A description of any assumptions or corrections, such as tests of normality and adjustment for multiple comparisons
☐	☒ A full description of the statistical parameters including central tendency (e.g. means) or other basic estimates (e.g. regression coefficient) AND variation (e.g. standard deviation) or associated estimates of uncertainty (e.g. confidence intervals)
☐	☒ For null hypothesis testing, the test statistic (e.g. *F*, *t*, *r*) with confidence intervals, effect sizes, degrees of freedom and *P* value noted *Give P values as exact values whenever suitable.*
☒	☐ For Bayesian analysis, information on the choice of priors and Markov chain Monte Carlo settings
☐	☒ For hierarchical and complex designs, identification of the appropriate level for tests and full reporting of outcomes
☐	☒ Estimates of effect sizes (e.g. Cohen's *d*, Pearson's *r*), indicating how they were calculated

Our web collection on statistics for biologists contains articles on many of the points above.

Software and code

Policy information about availability of computer code

Data collection	Cell Ranger (v7.1.0); xPonent (3.1 build 971); Diva (v 9.1) ; Isolight (v1.10.0)
Data analysis	Seurat (v4.0); DoubletFinder (v2.0), Harmony (v1.2), DESeq2 (1.42.0); GSEA (v4.3.3); FlowJo (v10.8.1); Prism (v10.3); Isospeak (v 2.9.0), scRepertoire v2.0.3 .

For manuscripts utilizing custom algorithms or software that are central to the research but not yet described in published literature, software must be made available to editors and reviewers. We strongly encourage code deposition in a community repository (e.g. GitHub). See the Nature Portfolio guidelines for submitting code & software for further information.

Data

Policy information about availability of data

All manuscripts must include a data availability statement. This statement should provide the following information, where applicable:

- Accession codes, unique identifiers, or web links for publicly available datasets
- A description of any restrictions on data availability
- For clinical datasets or third party data, please ensure that the statement adheres to our policy

All requests for additional raw and analyzed data should be directed to Andras Heczey. Patient-related data not included in the paper were generated as part of the clinical trial and may be subject to patient confidentiality. After removal of all human research subject identifiers, raw data for single-cell sequencing was deposited

in the Gene Expression Omnibus (GEO) under accession #GSE253352.

Research involving human participants, their data, or biological material

Policy information about studies with human participants or human data. See also policy information about sex, gender (identity/presentation), and sexual orientation and race, ethnicity and racism.

Reporting on sex and gender	Self-reported sex was collected and is listed in enrollment and outcome tables of the manuscript. Given the sample size of six in the CAR and twelve in the 15.CAR group (on DL2), sex / gender based analyses were not performed in this study.
Reporting on race, ethnicity, or other socially relevant groupings	Self-reported information on race and ethnicity were collected. Given the sample size of six in the CAR and twelve in the 15.CAR group (on DL2), race and ethnic-based analyses were not performed in this study.
Population characteristics	For the pediatric trials: children between 1 and 20 years old with GPC3+ solid tumors were enrolled. For the adult trials: patients between 30 and 2 years old with GPC3+ solid tumors were enrolled. Population based characteristics are reported in the patient characteristics tables together with corresponding biological variables for all patients on the study. Procurement eligibility: 1) Relapsed or refractory GPC3-positive solid tumors; 2) Age >1 year and ≤18 years; 3) Lansky or Karnofsky score >60%; 3) Life expectancy >16 weeks; 4) Child-Pugh- Turcotte score <7 (for patients with hepatocellular carcinoma only; 5) Informed consent explained to, understood by and signed by patient/guardian. Exclusion criteria for procurement: 1) History of hypersensitivity reactions to murine proteincontaining products OR presence of human anti-mouse antibody (HAMA) prior to enrollment (only patients who have received prior therapy with murine antibodies); 2) History of organ transplantation; 3) Known HIV positivity; 4) Severe previous toxicity from cyclophosphamide or fludarabine.
Recruitment	Recruitment was based on first-come / first-serve basis through self referral or by referring physician. After meeting eligibility, the patients were first enrolled on the procurement phase of the study enabling the generation of the CAR T cell products. After the product was manufactured and met release testing criteria, a separate informed consent was signed to enroll the patients on the treatment phase of the trials. We do not identify biases that could have impacted the presented results.
Ethics oversight	Clinical trials were reviewed and approved by the Protocol Review Committee, The Institutional Biosafety Committee, and the Institutional Review Board at Baylor College of medicine and the US Food and Drug Administration (FDA).

Note that full information on the approval of the study protocol must also be provided in the manuscript.

Field-specific reporting

Please select the one below that is the best fit for your research. If you are not sure, read the appropriate sections before making your selection.

☒ Life sciences ☐ Behavioural & social sciences ☐ Ecological, evolutionary & environmental sciences

For a reference copy of the document with all sections, see nature.com/documents/nr-reporting-summary-flat.pdf

Life sciences study design

All studies must disclose on these points even when the disclosure is negative.

Sample size	Sample size is based on the enrolled patients. All patients were included for all of the analyses. Data from four clinical trials are included: a total of 6 (3 on DL1 and 3 on DL2) patients enrolled on GAP NCT02932956, 6 patients (3 on DL1 and 3 on DL2) on GLYCAR NCT02905188, 8 patients on AGAR NCT04377932 and 4 patients on CATCH NCT05103631 are included in the manuscript.
Data exclusions	No data has been excluded from analysis
Replication	Serum cytokine, CAR and iC9.NGFR.IL15 transgene levels were measured in technical triplicates and means of technical triplicates are shown for each time-point. Cytotoxicity assessment was performed individually for each product using technical triplicates. Each patient serves as a biological replicate for all comparisons between CAR and 15.CAR cohorts.
Randomization	Patients were enrolled on single arm Phase 1 studies.; therefore, randomization is not applicable.
Blinding	Each trial was an open-label, single-arm, Phase 1 study; thus, blinding is not applicable as it cannot be performed.

Reporting for specific materials, systems and methods

We require information from authors about some types of materials, experimental systems and methods used in many studies. Here, indicate whether each material, system or method listed is relevant to your study. If you are not sure if a list item applies to your research, read the appropriate section before selecting a response.

Materials & experimental systems

n/a	Involved in the study
☐	☒ Antibodies
☐	☒ Eukaryotic cell lines
☒	☐ Palaeontology and archaeology
☒	☐ Animals and other organisms
☐	☒ Clinical data
☐	☒ Dual use research of concern
☒	☐ Plants

Methods

n/a	Involved in the study
☒	☐ ChIP-seq
☐	☒ Flow cytometry
☒	☐ MRI-based neuroimaging

Antibodies

Antibodies used

GPC3-and 15.GPC3-CAR T cell products and peripheral blood samples were assessed with flow cytometry using BUV395-Conjugated Mouse Anti-Human CD4 (Clone RPA-T4, Cat. No 564724), BUV496-Conjugated Mouse Anti-Human CD8 (Clone RPA-T8, Cat. No 612942), BUV 737-Conjugated Mouse Anti-Human TIM-3 (Clone 7D3, Cat. No 748820), BV421-Conjugated Mouse Anti-Human CD25 (Clone M-A251, Cat. No 562442), BV480-Conjugated Mouse Anti-Human CD45RO (Clone UCHL1, Cat. No 566143), BV650-conjugated Mouse Anti-Human CD279 (Clone MIH4, Cat. No 564324), BV711-conjugated Mouse-Anti-Human CD69 (Clone FN50, Cat. No 563836), BV786-Conjugated Mouse Anti-Human LAG3 (Clone T47-530, Cat. No 744727), BV605-Conjugated Mouse Anti-Human CD3 (Clone SK7, Cat. No 563219), APC-R700-Conjugated Mouse Anti-Human CD127 (Clone HIL-7R-M21, Cat. No 565185), FITC-Conjugated Mouse Anti-Human CD197 (CCR7) (Clone 150503, Cat. No 561271), BD Pharmingen™ PE-Conjugated Mouse Anti-Human CD271 (Clone C40-1457, Cat. No 557196), PerCP-Cy™5.5-Conjugated Mouse Anti-Human CD39 (Clone TU66, Cat. No 564899) and Viability Stain 780 (Cat. No 565388). PE-conjugated Mouse IgG1 k was used an isotype control (Cat. No 555749). All of the above antibodies are from BD Biosciences and had a dilution ratio of 1:20, except Anti-Human CD271 (1:10), IgG1 k (1:10) and Viability stain (1:1000).

Transduction efficiency of peripheral blood samples was assessed in products and peripheral blood via the following antibodies: GPC3-CAR expression was measured by Alexa Fluor® 647-Conjugated AffiniPure Goat Anti-Mouse IgG, F(ab')2 fragment specific (Polyclonal, Jackson Immunoresearch, Cat. No 115-605-006, 1:100 diluteion) and IL15 was measured by FITC-Conjugated Mouse Anti-Human NGFR (C40-1457, BD Biosciences, Cat. No 345104, 1:20 dilution). Nonspecific binding was mediated using Monoclonal Anti-Bovine IgG antibody (BG18, Sigma Aldrich, Cat. No B6901, 1:200 dilution).

iNKTs and NK cells were assessed using BUV395-Conjugated Mouse Anti-Human CD4 (Clone RPA-TP4, BD Biosciences, Cat. No 564724, 1:25 dilution), BUV496-Conjugated Mouse Anti-Human CD3 (Clone UCHT1, BD Biosciences, Cat. No 612940, 1:50 dilution), BUV805-Conjugated Mouse Anti-Human CD16 (Clone 3G8, BD Biosciences, Cat. No 748850, 1:50 dilution), BV421-Conjugated Mouse Anti-Human CD19 (Clone SJ25C1, BD Biosciences,Cat. No 659477, 1:50 dilution), BV480-Conjugated Mouse Anti-Human CD8 (Clone RPA-T8, BD Biosciences, Cat. No 566163, 1:50 dilution), BV750-Conjugated Mouse Anti-Human γδ TCR (Clone 11F2, Cat. No 747127 1:50 dilution), FITC-Conjugated Mouse Anti-Human TCR-α/β (Clone WT 31, Cat. No 347773, 1:10 dilution), PE-Conjugated Mouse Anti-Human iNKT (Clone 6B11, BD Biosciences,Cat. No 552825, 1:10 dilution), PerCP Cy5.5-Conjugated Mouse Anti-Human CD14 (Clone MΦP9, Cat. No 562692, 1:50 dilution), APC-R700-Conjugated Mouse Anti-Human CD56 (Clone NCAM16.2, Cat. No 565139, 1:20 dilution), Brilliant Stain Buffer Plus (Cat. No 566385, 1:20 dilution), and Viability Stain 780 (Cat. No 565388, 1:1000 dilution) and APC-Conjugated Mouse Anti-Human Vβ11 (Clone C21, Cat. No A66905, 1:12.5 diltuion). All of the above antibodies are from BD Biosciences, except Vβ11 which is from Beckman Coulter Life Sciences.

Validation

All antibodies are commercially available and have been validated in previous studies., including in PMID: 31953246. However, all commercially available flow cytometry antibodies were additionally tested on both healthy donor PBMCs and purified human GPC3-CAR+ Ts prior to use on patient PBMCs.

Eukaryotic cell lines

Policy information about cell lines and Sex and Gender in Research

Cell line source(s)	HUH7 (originated from a male patient and a gift from Xiaotong Song), available from commercial vendors. PG13 producer murine fibroblast cell line was obtained from the American Type Culture Collection, is used and maintained in the cGMP facility of the Texas Children's Hospital according to FDA regulations.
Authentication	All cell lines were STR fingerprinted at MD Anderson Cancer Center within one year of use
Mycoplasma contamination	All cell lines were checked for mycoplasma contamination (Lonza MycoAlert) every two months and tested negative.
Commonly misidentified lines (See ICLAC register)	No commonly misidentified cell lines used in this study

Clinical data

Policy information about clinical studies

All manuscripts should comply with the ICMJE guidelines for publication of clinical research and a completed CONSORT checklist must be included with all submissions.

Clinical trial registration	Two Phase I clinical trials with second-generation GPC3-specific CAR to treat pediatric (GAP: NCT02932956) and Adult (GLYCAR: NCT02905188) patients. And two phase-1 clinical trials utilizing GPC3-specific CAR co-expressing IL-15 to treat pediatric (AGAR: NCT04377932) and adult (CATCH: NCT05103631) patients.
Study protocol	Study Protocols are included as supplementary materials.
Data collection	All data for the pediatric trials were collected at Texas Children's Hospital, Houston TX and all data for the adult trials were collected at Houston Methodist Hospital. Patients were recruited for GAP from Sept 2019 to Dec 2021, GLYCAR from Feb 2020 to June 2022, AGAR from Dec 2021 to Feb 2023 and CATCH from June 2022 to Jan 2023. Data was collected based on the study calendar and included H&P, clinical labs (CBC w diff, chem 10, AST, T bili), peripheral blood samples (Day -4, Day 0, Week 1, 2, 3, and 4) and tumor biopsy (week 2 post-infusion only). For Extended data figure 1A, original microscopic images were collected at the Children's Hospital of Philadelphia 12/2017. All other data for correlative studies were collected, analyzed and interpreted at Texas Children's Hospital.
Outcomes	Primary outcome: Safety and defining the maximum tolerated dose. Adverse events were collected from Day -4 to Day +28 and were graded according to the Common Terminology Criteria of Adverse Evens v5 (CTCAEv5) of the National Cancer Institute. Secondary Outcome: Antitumor responses were measured by comparing pre and post-infusion imaging studies. Other outcome measures: immunologic responses of CAR T cells. Peripheral blood and biopsy samples collected as described above. Please, see attached protocols for further details on outcome measures.

Plants

Seed stocks	N/A
Novel plant genotypes	N/A
Authentication	N/A

Flow Cytometry

Plots

Confirm that:

☒ The axis labels state the marker and fluorochrome used (e.g. CD4-FITC).

☒ The axis scales are clearly visible. Include numbers along axes only for bottom left plot of group (a 'group' is an analysis of identical markers).

☒ All plots are contour plots with outliers or pseudocolor plots.

☒ A numerical value for number of cells or percentage (with statistics) is provided.

Methodology

Sample preparation	Patient PBMCs were isolated from peripheral blood by density gradient centrifugation the washed in 1x PBS prior to staining. Cryopreserved T cells were thawed in RPMI media and spun to remove freezing medium and washed in 1x PBS prior to staining the cells.
Instrument	BD LSRII five-laser flow cytometer and BD Symphony A5 flow cytometer
Software	Flow cytometry samples were collected using BD FACSDiva software version 9.1 and analyzed using FlowJo 10.8.1
Cell population abundance	Stain between 0.1 - 1x10e6 PBMC cells per timepoint, depending on cell number availability. Stained 1x10e6 cells of the infusion product.
Gating strategy	For pre-infusion CAR T cell products and post-infusion peripheral blood mononuclear cells (PBMCs), the lymphocyte region was selected on forward and side scatter, followed by singlets gate using FSC-H vs FSC-A. Live cells were gated using 780 stain vs SSC. Next we gated CD3 positive cells using CD3 vs SSC. CAR+ and NGFR+ cells were gated using CAR vs SSC-A and NGFR vs

SSC-A. CAR and NGFR isotypes were used as a negative control where additional cells were available. For the products, we gated on CD4+ and CD8+ cells from the CAR +gate and we looked at the expression of various exhaustion/activation markers (CCR7, CD45RO, TIM-3, LAG-3, PD-1, CD39 and CD69). FMOs panels for the markers were used to set the gates. For assessment of other lymphocytes in PBMCs after infusion, the lymphocyte region was selected on forward and side scatter, followed by selection of either CD3+ or CD3- subsets using CD3 vs SSC. The CD3+ subset was evaluated for the iNKT cells using both an iNKT antibody specific for the invariant iNKT TCR and the Vbeta11 antibody. The CD3- subset was evaluated for NK subsets by staining for both CD56 and CD16.

☒ Tick this box to confirm that a figure exemplifying the gating strategy is provided in the Supplementary Information.